PHYSICAL REVIEW A VOLUME 22, NUMBER 5 NOVEMBER 1980

Theory of coherences produced by radiatively assisted inelastic collisions: Weak-field impact-core limit

Paul R. Berman

*Laboratoire Aimé Cotton, Centre National de la Recherche Scientifique II, Bâtiment 505, 91405 Orsay-Cedex, France and Physics Department, New York University, 4 Washington Place, New York, New York 10003**

(Received 21 March 1980)

A theoretical calculation of the final-state coherences produced by a radiatively assisted inelastic collision (RAIC) is presented. Two atoms, A and A', collide in the presence of an external radiation field to produce the RAIC reaction $A_i + A_{i'} + \hbar\Omega \rightarrow A_f + A_{f'}$, where $|ii'\rangle$ is the initial state, $|ff'\rangle$ is the final state, and Ω is the frequency of the external field. It is assumed that the final states consist of a number of nearly degenerate levels and the coherences produced in these levels by the RAIC reaction is calculated. These final-state coherences can be monitored by standard techniques (polarization of fluorescence, quantum beats) enabling one to use the final-state coherences as a probe of the RAIC reaction. The calculation is limited to the weak-field (perturbation-theory) limit and is valid only in the impact core of the RAIC profile.

I. INTRODUCTION

In a previous paper[1] (to be referred to as RAIC I), a general theory or radiatively assisted inelastic collisions (RAIC) was developed. These collisions represent processes of the form

$$A_i + A_i' + \hbar\Omega \rightarrow A_f + A_f',$$

in which two atoms (A and A') are excited from initial states ii' to final states ff' by the combined action of the collision and the absorption of a photon from an external pulsed radiation field. Whereas most previous theories of RAIC considered only one possible excitation channel (from non degenerate state ii' to nondegenerate state ff'), the theory presented in RAIC I allowed for the more general RAIC excitation from a group of initial levels characterized by some appropriate density matrix to a group of final levels. An expression was obtained for the final-state density matrix which completely described both the population and coherence properties of the excitation process. The final-state coherences can be monitored by standard experimental techniques (e.g., measurement of the polarization of fluorescence or quantum beats originating from the final states of one of the atoms); alternatively, one can monitor the final-state populations (e.g., by measuring the total fluorescence rate from one of the final states). It turns out, however, that measurements of final-state coherences provide a more sensitive probe of the RAIC interatomic potentials than do measurements of final-state populations. Thus, it appears useful to develop a theory of RAIC which permits one to calculate the induced-final-state coherences.

In this paper, a perturbative solution of the RAIC equations is obtained which is valid provided (1) the external field is sufficiently weak and (2) the detunings are restricted to the impact core of the RAIC profile. Starting with some arbitrary initial density matrix and assuming interatomic potentials and external-field polarizations of a quite arbitrary nature, the final-state density matrix for the system is calculated. The most general case leads to rather lengthy expressions which are presented in the Appendices. Specific results are given in the body of the paper for the reduced density matrix of atom A' in the limits of (1) dipole-dipole interatomic potential, (2) straight-line collisional trajectory, (3) linearly polarized external field, (4) central tuning, (5) unpolarized initial state, (6) final states of a given atom characterized by the same J quantum number, and (7) a summation over intermediate virtual states that reduces to one term, owing to a nearly satisfied resonance condition. It is shown that the fluorescence emitted from the final states of one of the atoms directly reflects the nature of the interatomic potential. Thus, in contrast with normal RAIC experiments where one must record an entire RAIC profile as a function of detuning to test interatomic potentialmodels, a polarization measurement at central tuning (where the signal is largest) serves to probe the interatomic potential.

It may seem strange that collisions *induce* coherence, since it is generally thought that collisions *destroy* coherence. In fact, it will be seen that the collisional interaction may be viewed as two unpolarized (but possibly correlated) "fields" incident on the atoms from all directions. The fields are chosen to have the same multipolar properties as the collisional interactions they represent (e.g., a dipole operator is replaced by a dipole field). In this way the final-state coher-

ence can be understood as the combined action of *three* fields; two unpolarized fields plus the external field. It is the external field which may be polarized and possesses a well-defined directionality in any case, that is the origin of the final-state coherence. The collisional interaction responsible for the RAIC reaction will, in general, modify the final-state coherence.

In Sec. II, the physical system is described and an expression for the final-state amplitude given. An outline of the calculation is presented in Sec. III, with the details given in the Appendices. The final-state density matrix is given in Sec. IV for the case outlined above. In Sec. V the RAIC excitation cross sections and the polarization of the fluoresence emitted from the final state of atom A' are calculated using a cutoff procedure to treat collisions with small impact parameters. A discussion and physical interpretation of the results are given in Sec. VI.

It should be noted that this paper is essentially self-contained. However, the reader is referred to RAIC I for a general overview of the problem, for a detailed derivation of the RAIC equations including validity conditions, and for references to previous work.

II. PHYSICAL SYSTEM AND TRANSITION AMPLITUDE

The physical system consists of two atoms, A and A', undergoing a collision in the presence of a pulsed radiation field. The time of closest approach during the collision is $t=t_c$ and the center-of-mass position of the atoms at this time is $\vec{R}=\vec{R}_c$. The amplitude of the pulsed field is assumed to vary slowly during the collision and is evaluated at $(\vec{R}_c, t_c)$; the field is taken to be of the form

$$\vec{E}(t;\vec{R}_c,t_c)=\tfrac{1}{2}[\vec{\mathcal{E}}_c e^{-i\Omega t}+\vec{\mathcal{E}}_c^{*} e^{i\Omega t}], \tag{1}$$

where $|\vec{\mathcal{E}}_c|$ is the field amplitude at $(\vec{R}_c, t_c)$.

The energy levels of atoms A and A' are shown in Fig. 1. Each label in the figure represents a group of levels having a maximum frequency separation $\omega_\epsilon \ll \tau_c^{-1}$, where τ_c is the duration of a collision. Since

$$\omega_\epsilon \tau_c \ll 1, \tag{2}$$

levels within a given group may be considered as degenerate during the RAIC. The levels associated with atom A are represented by lower-case unprimed variables and those associated with atom A' by primed ones. A capital letter refers to a state of the composite system ($I=i\,i'$, $E=e\,e'$, $F_1=f_1 f_1'$, etc.) and the convention

$$\omega_I=\omega_i+\omega_{i'},\quad \omega_F=\omega_f+\omega_{f'}, \tag{3}$$

etc., is adopted, where $\omega_\alpha=E_\alpha/\hbar$ and E_α is the energy associated with state α.

Before the collision, the atoms are in an arbitrary linear superposition of the states $|I\rangle = |ii'\rangle = |i\rangle|i'\rangle$, where i and i' represent any of the levels in the i and i' groups, respectively. The field is assumed to be nearly resonant with the $I \rightarrow F$ transition in the composite system, i.e., $\Omega \approx \omega_F - \omega_I$. More precisely, the detuning Δ defined by

$$\Delta=\Omega-\omega_{FI}, \tag{4}$$

$$\omega_{FI}=\omega_F-\omega_I \tag{4a}$$

is limited, in this work, to the impact core of the RAIC profile

$$|\Delta|\,\tau_c \ll 1. \tag{5}$$

All other atom-atom or atom-field interactions are assumed to be nonresonant; in other words, all levels outside the I and F groups enter the problem only as *virtual* levels. The contribution of these virtual levels can be included in effective operators that act in the IF subspace only. The problem is to determine the final-state density matrix following the collision since it provides a complete description of the final-state coherences and populations produced by RAIC.

The RAIC can be characterized by three operators which have been discussed in RAIC I. First, there is the "light-shift" operator $\hat{S}_L$ which couples and shifts the levels *within* both the initial and final groups of levels. This light-shift operator represents the virtual excitation and de-excitation of either of the atoms by the external field. The effects produced by $\hat{S}_L$, which are second order in the field, are neglected in this work, since the field is treated in a perturbation-theory limit.

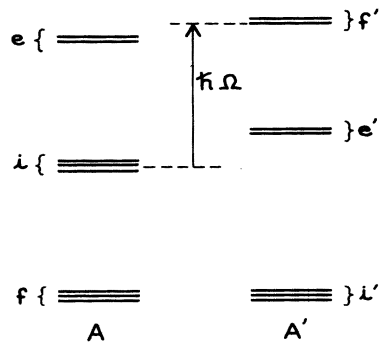

FIG. 1. Energy-level diagram of atoms A and A'. Each group of levels labeled by a single letter is nearly degenerate with a maximum frequency spacing between levels within a group less than an inverse collision time. The external-field frequency Ω is such that $\hbar\Omega \approx (E_f + E_{f'}) - (E_i + E_{i'})$.

Second, there is the collisional operator $\hat{S}_c$ which also couples and shifts the levels *within* the initial and final groups of levels. This operator is second order in the collisional interaction, representing the collision-induced virtual excitation and de-excitation of the composite AA' system in either its initial or final state. The operator $\hat{S}_c$ is the origin of the pressure broadening and shifting of spectral profiles. The relative importance of $\hat{S}_c$ is dependent on (i) the detuning Δ and (ii) the impact parameter associated with a given collision. Owing to condition (5), the collision possesses sufficient frequency components to effectively compensate for the detuning Δ. Thus, in contrast to the case $|\Delta|\tau_c > 1$, where collisional shifts can significantly enhance excitation cross sections by bringing the atomic transition frequency into instantaneous resonance with the field, all effects produced by the operator $\hat{S}_c$ related to the detuning may be neglected. The dependence of $\hat{S}_c$ on the impact parameter is discussed following the description of the transition operator.

The transition operator $\hat{T}(IF)$ represents the combined action of the (field + collision) in *coupling* the initial state $|I\rangle$ to final state $|F\rangle$ via a virtual excitation of intermediate states. This operator can be represented diagrammatically by the four terms shown in either Fig. 2 or Fig. 3. In Figs. 2(a) and 3(a), the collision (represented by non-wavy lines) acts to virtually excite the atoms from state $|ii'\rangle$ to state $|ef'\rangle$ and the field (represented by wavy lines) then acts on atom A to complete the excitation to the final state $|ff'\rangle$. In Figs. 2(b) and 3(b) the collision excites the virtual state $|fe'\rangle$ and the field acts on atom A' to complete the excitation. In Figs. 2(c) and 3(c) the field acts on atom A to excite the virtual state $|ei'\rangle$ and the collision completes the excitation to the final state $|ff'\rangle$. Finally, in Figs. 2(d) and 3(d), the field acts on atom A' to excite the virtual state $|ie'\rangle$ and the collision completes the excitation.

It may be seen from Fig. 2 that the transition operator is linear in both the field and collisional interaction. Explicitly,[1] one finds matrix elements of $\hat{T}(IF)$ to be

$$\langle F|\hat{T}(IF;t,b,v_r,\Theta,\vec{R}_c,t_c)|I\rangle = \frac{1}{2\hbar}\left(\frac{\langle F|\vec{\mu}_T|E\rangle\langle E|\mathcal{U}(\vec{R}(t))|I\rangle}{\omega_{EI}} + \frac{\langle F|\mathcal{U}(\vec{R}(t))|E\rangle\langle E|\vec{\mu}_T|I\rangle}{\omega_{EF}}\right)\cdot\vec{\mathcal{E}}_c\ , \quad (6)$$

where t is the time during the collision; b, v_r,

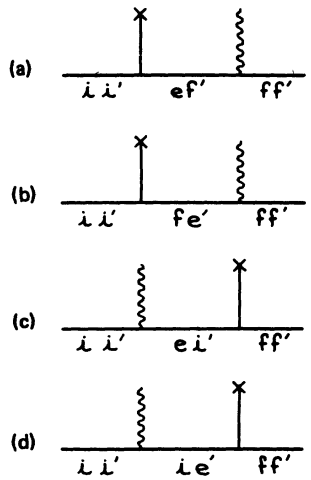

FIG. 2. Diagrams representing matrix elements of the transition operation from initial state $|ii'\rangle$ to final state $|ff'\rangle$. A straight-line vertex corresponds to a collision interaction and wavy-line vertex to an atom-field interaction. The states e and e' represent some arbitrary intermediate (virtual) states in atoms A and A', respectively.

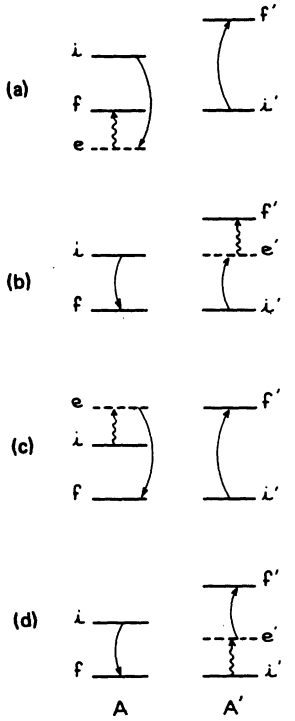

FIG. 3. A schematic representation of the contributions to the final-state RAIC amplitude complementary to that shown in Fig. 2. Each diagram corresponds to the similarly labeled diagram in Fig. 2. Solid lines with arrows represent the collisional interaction and wavy lines represent the atom-field interaction. States e and e' are virtual states excited in the RAIC reaction. Each level actually corresponds to a group of nearly degenerate levels.

and Θ are the impact parameter, relative speed, and collision orientation, respectively, associated with the collision

$$\vec{\mu}_T = \vec{\mu} + \vec{\mu}' \tag{7}$$

where $\vec{\mu}$ and $\vec{\mu}'$ are the electric-dipole operators for atoms A and A', respectively; and $\mathcal{U}(\vec{R}(t))$ is the collision interaction Hamiltonian calculated assuming a classical interatomic collision trajectory $\vec{R}(t)$. In writing Eq. (6), I have used the fact that $\omega_\epsilon \ll \omega_{EI}$, ω_{EF} (recall that ω_ϵ is the maximum frequency separation within a group of levels) and have adopted a summation convention in which any repeated state label (*not* including its appearance in a phase factor or frequency denominator) is summed over (e.g., in Eq. (6), there is a sum over E but not over I or F).[2] Since $\vec{\mu}_T$ is the sum of two terms, one can readily identify Eq. (6) with the four figures of Fig. 2. An analogous calculation for the operator $\hat{T}(FI)$ yields

$$\langle I|\hat{T}(FI;t)|F\rangle = \langle F|\hat{T}(IF;t)|I\rangle^* . \tag{8}$$

Since $\hat{T}(IF)$ varies linearly in $\mathcal{U}$ and $\hat{S}_c$ varies as $(\mathcal{U})^2$, and since $\mathcal{U}$ varies typically as b^{-n} $(n>0)$, one can conclude that, for collisions with "large" impact parameters, the effects produced by $\hat{S}_c$ may be neglected in comparison with those produced by $\hat{T}(IF)$. For "smaller" impact parameters, the contribution of $\hat{S}_c$ can no longer be ignored. For the present, I consider only those collisions with $b>b_0$, where b_0 is the minimum impact parameter for which the contribution from $\hat{S}_c$ can be neglected. In Sec. V a simple model is developed for treating collisions with $b<b_0$.

Thus, during collisions with $b>b_0$, the probability amplitudes (in the interaction representation) for the initial and final states obey the equations of motion

$$i\hbar\dot{a}_F = \langle F|T(IF,t)|I\rangle e^{-i\Delta t}a_I , \tag{9a}$$

$$i\hbar\dot{a}_I = \langle F|\hat{T}(IF,t)|I\rangle^* e^{i\Delta t}a_F , \tag{9b}$$

where it has been assumed that changes in a_I or a_F resulting from level decay and atomic motion (Doppler effect) are negligible on the time scale of a collision. Furthermore, it is now assumed that the field strength is weak enough so that Eqs. (9) can be solved by perturbation theory with initial conditions $a_I(t_c^-)\neq 0$, $a_F(t_c^-)=0$, where t_c^- is a time just before the collision. Integrating Eqs. (9) in the perturbation-theory limit, one finds a final-state amplitude at time t_c^+ just following the collision given by

$$a_F(t_c^+) = (i\hbar)^{-1}\left(\int_{t_c^-}^{t_c^+}\langle F|\hat{T}(IF,t)|I\rangle e^{-i\Delta t}dt\right)a_I(t_c^-) . \tag{10}$$

Perturbation theory is valid provided that $|a_F(t)|^2 \ll 1$ for all t during a collision having $b=b_0$. Under typical experimental conditions, perturbation theory is valid for power densities $\lesssim 10^{10}\mathrm{W/cm^2}$.

It remains to carry out the integration in Eq. (10), to form final-state density-matrix elements, and to average over all appropriate collision parameters.

III. OUTLINE OF CALCULATION

Forming final-state density-matrix elements from the amplitude (10) and carrying out the average over collision orientations Θ, one obtains[3]

$$\rho_{FF_1}(t_c^+;b,v_r,\vec{R}_c,t_c) = R^{II_1}_{FF_1}(b,v_r,\vec{R}_c,t_c)\rho_{II_1}(t_c^-), \tag{11a}$$

where

$$R^{II_1}_{FF_1}(b,v_r,\vec{R}_c,t_c) = \hbar^{-2}(8\pi^2)^{-1}\int d\Theta\int_{t_c^-}^{t_c^+}\langle F|\hat{T}(IF,t)|I\rangle e^{-i\Delta t}dt\int_{t_c^-}^{t_c^+}\langle F_1|\hat{T}(IF,t')|I_1\rangle^* e^{i\Delta t'}dt' . \tag{11b}$$

The dependence of $\hat{T}$ on $(b,v_r,\Theta,\vec{R}_c,t_c)$ has been suppressed in Eqs. (10) and (11). In this section, a method for evaluating Eqs. (11) is outlined; details of the calculation are given in the Appendices. The averaging over b and $\vec{R}_c$ is deferred to Sec. V.[4]

The matrix elements of $\hat{T}$ needed in Eq. (11b) may be calculated using Eq. (6) once the interatomic potential $\mathcal{U}$ and the field $\vec{\mathcal{E}}_c$ are specified. An arbitrary potential can be written in the form

$$\mathcal{U}(t-t_c,\ b,v_r,\Theta) = A^{kk'}_{qq'}(t-t_c,b,v_r,\Theta)T^k_q\,T'^{k'}_{q'}, \tag{12}$$

where T^k_q and $T'^{k'}_{q'}$ are components of irreducible tensor operators of rank k and k' (assumed integral), respectively, which act on states of atoms A and A', respectively. In the form (12), the potential can be viewed as the sum of correlated multipolar fields acting on each of the atoms, the correlation provided by the coupling constants

$A^{kk'}_{qq'}$. The average over all collision orientations needed in Eq. (11b) is equivalent to including all possible directions of incidence and polarizations for these multipolar fields. In some sense, therefore, the collisions can be viewed as producing the same effect as a sum of unpolarized, but correlated, multipolar fields acting on atoms A and A'. This picture of the collisional process can be useful in understanding the coherences produced by RAIC and is used in Sec. VI to help explain the results obtained for the various RAIC cross sections.

In order to carry out the average over Θ, it is convenient to rewrite Eq. (12) in the form

$$\mathfrak{A}(t-t_c;b,v_r,\Theta)={}^{kk'}A^K_Q(t-t_c;b,v_r,\Theta)\,{}^{kk'}V^K_Q\,, \tag{13}$$

where

$${}^{kk'}V^K_Q=\begin{bmatrix} k & k' & K \\ q & q' & Q \end{bmatrix} T^k_q\,T^{\prime k'}_{q'}\,, \tag{14a}$$

$${}^{kk'}A^K_Q=\begin{bmatrix} k & k' & K \\ q & q' & Q \end{bmatrix} A^{kk'}_{qq'}\,, \tag{14b}$$

and the quantity in brackets is a Clebsch-Gordon coefficient. Since the V^K_Q transform as the components of an irreducible tensor operator under rotation, the expansion coefficients A^K_Q transform as

$${}^{kk'}A^K_Q(t-t_c;b,v_r,\Theta)$$
$$={\mathfrak{R}^{(K)}_{QQ'}}^{*}(\Theta)\,{}^{kk'}A^K_{Q'}(t-t_c;b,v_r,0)\,, \tag{15}$$

where the $\mathfrak{R}^{(K)}_{QQ'}$ are matrix elements of the irreducible representation of order (K) of the rotation group and $\Theta=0$ is some arbitrary collision geometry. The Θ dependence is now contained totally in the $\mathfrak{R}^{(K)}_{QQ'}$, enabling one to easily perform the Θ integration required in Eq. (11b) (see below). In anticipation of the time integrals also required in Eq. (11b), I define the quantities

$$A^{kk'}_{qq'}(b,v_r,\Theta;\Delta)=(v_r/b)\int_{t_c^- - t_c}^{t_c^+ - t_c} A^{kk'}_{qq'}(\tau,b,v_r,\Theta)\times e^{-i\Delta(\tau+t_c)}\,d\tau \tag{16a}$$

and

$${}^{kk'}A^K_Q(b,v_r,\Theta;\Delta)=(v_r/b)\int_{t_c^- - t_c}^{t_c^+ - t_c} {}^{kk'}A^K_Q(\tau,b,v_r,\Theta)\times e^{-i\Delta(\tau+t_c)}\,d\tau\,, \tag{16b}$$

which are also related via Eq. (14b). Equation (15) remains valid for ${}^{kk'}A^K_Q(b,v_r,\Theta;\Delta)$.

It remains to specify the atom-field interaction $\vec{\mu}_T\cdot\vec{\mathcal{E}}_c$. The field amplitude may be written

$$\vec{\mathcal{E}}_c=\hat{\epsilon}\,\mathcal{E}_c\,,\quad |\hat{\epsilon}|=1 \tag{17}$$

where $\hat{\epsilon}$ is a complex polarization vector. One then finds

$$\vec{\mu}_T\cdot\vec{\mathcal{E}}_c=(-1)^q(\mu_T)^{(1)}_q\,\epsilon_{-q}\,\mathcal{E}_c\,, \tag{18}$$

where

$$\epsilon_1=-(\epsilon_x+i\epsilon_y)/\sqrt{2}\,,$$
$$\epsilon_{-1}=(\epsilon_x-i\epsilon_y)/\sqrt{2}\,, \tag{19}$$
$$\epsilon_0=\epsilon_z\,,$$

and

$$(\mu_T)^{(1)}_1=-[(\mu_T)_x+i(\mu_T)_y]/\sqrt{2}\,,$$
$$(\mu_T)^{(1)}_{-1}=[(\mu_T)_x-i(\mu_T)_y]/\sqrt{2}\,,\quad (\mu_T)^{(1)}_0=(\mu_T)_z\,. \tag{20}$$

The quantities $(\mu_T)^{(1)}_q$ are the components of an irreducible tensor operator of rank 1.

Since all the operators appearing in Eq. (6) have now been expressed in terms of the components of irreducible tensor operators, the matrix elements appearing in Eq. (6) are easily calculated using the Wigner-Eckart theorem[5] (see Appendix A). The resulting expressions for $\langle F|\,T(IF,t)|I\rangle$ and $\langle F_1|\,T(IF,t)|\,I_1\rangle^*$ are then inserted into Eq. (11b) and the integration over Θ is performed using the fact that[6]

$$(8\pi^2)^{-1}\int d\Theta\,\mathfrak{R}^K_{QQ'}(\Theta)\,(\mathfrak{R}^{\bar{K}}_{\bar{Q}\bar{Q}'}(\Theta))^*$$
$$=(2K+1)^{-1}\,\delta_{K\bar{K}}\delta_{Q\bar{Q}}\delta_{Q'\bar{Q}'} \tag{21}$$

to arrive at a value for $R^{II_1}_{FF_1}(b,v_r,\vec{R}_c,t_c)$ [Eq. (11b)] and $\rho_{FF_1}(t_c^+;b,v_r,\vec{R}_c,t_c)$ [Eq. (11a)]. The final expressions are rather lengthy and are given in Appendix A along with the details of the calculation.

Experimentally, one often observes the final-state properties of only one of the atoms. Imagine, for example, that one monitors the final-state coherence of atom A'. Mathematically, this coherence is described by the reduced density matrix obtained by tracing ρ_{FF_1} over the final-state variables of atom A. Explicitly, these reduced density-matrix elements $\rho_{f'f'_1}$ are given by setting $F=ff'$, $F_1=ff'_1$ and summing over f, i.e.,

$$\rho_{f'f'_1}(t_c^+;b,v_r,\vec{R}_c,t_c)=\rho_{ff';ff'_1}(t_c^+;b,v_r,\vec{R}_c,t_c)\,. \tag{22}$$

A calculation of these reduced matrix elements, those of atom A, and the connection between the two is also given in Appendix A.

The coherence properties of a system are conveniently expressed in terms of the irreducible tensor components of the density matrix. The transformation between matrix elements is given by

$$ {}^{f'f'_1}\rho'^{K}_{Q} = (-1)^{J_{f'_1}-m_{f'_1}} \begin{bmatrix} J_{f'} & J_{f'_1} & K \\ m_{f'} & -m_{f'_1} & Q \end{bmatrix} \times \langle f' J_{f'} m_{f'} | \rho' | f' J_{f'_1} m_{f'_1} \rangle , \tag{23a} $$

along with the inverse transform

$$ \langle f' J_{f'} m_{f'} | \rho' | f' J_{f'_1} m_{f'_1} \rangle = (-1)^{J_{f'_1}-m_{f'_1}} \begin{bmatrix} J_{f'} & J_{f'_1} & K \\ m_{f'} & -m_{f'_1} & Q \end{bmatrix} {}^{f'f'_1}\rho'^{K}_{Q} , \tag{23b} $$

where it has been assumed that a state $|\alpha\rangle$ may be labeled by $|\alpha J_\alpha m_\alpha\rangle$ and that states within a given group of levels differ only in their J and m_J quantum numbers.[7] The ρ^K_Q are matrix elements of the density matrix expanded in an irreducible tensor basis. When expressed in this fashion, one can see directly if there is any final-state coherence. The quantity ρ^0_0 is given by

$$ {}^{f'f'_1}\rho'^{0}_{0} = (2J_{f'}+1)^{-1/2} \langle f' J_{f'} m_{f'} | \rho' | f' J_{f'} m_{f'} \rangle \delta_{J_{f'} J_{f'_1}} \tag{24} $$

and is proportional to the total final-state *population*. Any nonzero value of ρ'^K_Q for $K>0$ indicates that final-state coherence exists, since a totally unpolarized final state leads to $\rho'^K_Q = 0$ for $K \neq 0$.

In Appendix A, general expressions for $\rho'_{f'f'_1}$ and ρ'^K_Q are obtained, assuming an arbitrary initial state. These expressions are evaluated in detail in Appendix B for the case of an unpolarized initial state. In the following section, certain limiting cases of these calculations are discussed.

IV. RESULTS FOR A SPECIFIC MODEL

In order to illustrate the physical principles involved in the RAIC process, I consider a limiting case of the general results presented in Appendices A and B. The following model is adopted: (1) Each group of levels α can be represented by a single angular momentum quantum number J_α (valid for fine-structure splittings $> \tau_c^{-1}$). (2) The initial state is unpolarized. (3) Owing to a nearly satisfied resonance condition, only *one* group of levels enters in the summation over intermediate virtual states. In this limit, the reduced density matrix for atom A' is calculated. Since the final state of atom A' is characterized by a single J value $J_{f'} = J_{f'_1}$, the calculation of ${}^{f'f'}\rho'^{K}_{Q}$ is essentially one in which the Zeeman coherences of level f' are determined.

In order for condition (3) to be satisfied *one* of the virtual levels shown in Fig. 3 must be nearly coincident with a real atomic level. This condition can be achieved with any of the level schemes shown in Fig. 4. For example, if the level scheme is as shown in Fig. 4(a), then the dominant contribution to the final-state amplitude comes from the diagram of Fig. 2(a) with the sum over intermediate states e restricted to the single group of states $e=r$; contributions from states $e \neq r$ as well as from the other diagrams of Figs. 2(b)–2(d) are relatively unimportant in this case in comparison with this nearly resonant contribution. Similarly, if the level scheme is as shown in Figs. 4(b)–4(d), the dominant contribution comes from the diagrams of Figs. 2(b)–2(d) with the summation over intermediate states restricted to $e=r$ or r'.

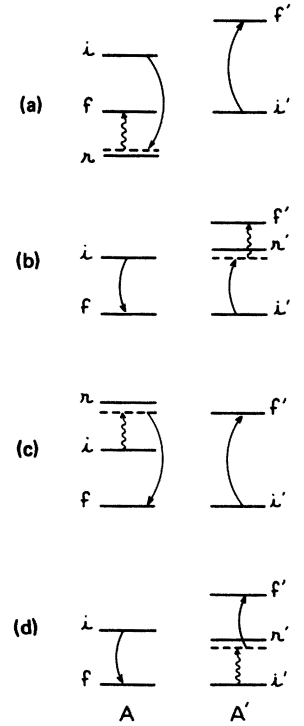

FIG. 4. Four different cases of energy-level schemes that lead to a single term dominating the sum over intermediate virtual states. Each level corresponds to a group of nearly degenerate levels.

The frequency mismatches associated with Figs. 4(a)–4(d) are

$$\Delta_a = \omega_r + \omega_{f'} - \omega_I \ , \tag{25a}$$

$$\Delta_b = \omega_f + \omega_{r'} - \omega_I \ , \tag{25b}$$

$$\Delta_c = \omega_r + \omega_{i'} - \omega_F \ , \tag{25c}$$

$$\Delta_d = \omega_i + \omega_{r'} - \omega_F \ , \tag{25d}$$

respectively. Although these frequencies are small in comparison with those associated with other virtual states, they still are assumed to satisfy $|\Delta_\alpha|\tau_c \gg 1$ ($\alpha = a - d$) to ensure that states r or r' still act as virtual states in the RAIC process. Experimentally, one often seeks level schemes similar to those shown in Fig. 4 in order to enhance excitation probabilities.

For the level scheme of Fig. 4(a), the final-state reduced density matrix for atom A' is obtained from Eqs. (B3), (B4), and (25a) as

$$\begin{aligned}{}^{ff'}\rho_Q'^K(t_c^+; b, v_r, \vec{R}_c, t_c)_a = (b\mathcal{E}_c/\hbar v_r)^2 N_I^{-1\,kk'} A_{Q'}^{K'}(b, v_r, 0; \Delta)[{}^{pp'}A_{Q'}^{K'}(b, v_r, 0; \Delta)]^* \\ \times P_{KQ}\Delta_a^{-2}(-1)^{J_f - J_{f'} - J_i - J_{i'} + K' + p' + k'} |\langle f\|\mu^{(1)}\|r\rangle|^2 \langle r\|T^{(k)}\|i\rangle \\ \times \langle r\|T^{(p)}\|i\rangle^* \langle f'\|T'^{(k')}\|i'\rangle \langle f'\|T'^{(p')}\|i'\rangle^* \begin{Bmatrix} 1 & 1 & K \\ J_r & J_r & J_f \end{Bmatrix} \\ \times \begin{Bmatrix} k & p & K \\ J_r & J_r & J_i \end{Bmatrix} \begin{Bmatrix} k' & p' & K \\ p & k & K' \end{Bmatrix} \begin{Bmatrix} k' & p' & K \\ J_{f'} & J_{f'} & J_{i'} \end{Bmatrix}, \end{aligned} \tag{26}$$

where N_I is the number of initial states,

$$P_{KQ} = (-1)^{Q_s} \epsilon_j^* \epsilon_s \begin{bmatrix} 1 & 1 & K \\ Q_j & -Q_s & Q \end{bmatrix}, \tag{27a}$$

$\langle \| \cdots \| \rangle$ is a reduced matrix element, $\{\cdots\}$ is a 6-J symbol, and

$$Q_1 = 1 \ , \ Q_{-1} = -1 \ , \ Q_0 = 0 \tag{27b}$$

as defined in Eq. (A17).

Equation (26) has a simple interpretation in terms of Fig. 4(a). The collision excites the atoms from state ii' to virtual state rf'; this process is represented by the product of the ${}^{kk'}A_{Q'}^{K'}[{}^{pp'}A_{Q'}^{K'}]^*$ factor and the reduced matrix elements of the collision operators T^k, T^p, $T^{k'}$, $T'^{p'}$. The field then acts on atom 1 to excite the system from state rf' to state ff'; this process is represented by the factor $P_{KQ}|\langle f\|\mu^{(1)}\|r\rangle|^2$, with P_{KQ} containing the polarization properties of the field. The 6-J and Clebsch-Gordon coefficients which appear are geometrical factors which arise when the various J levels are coupled by either the collisional interaction or the field.

For the level scheme shown in Fig. 4(b), the result is given by Eqs. (B3), (B6), and (25b) as

$$\begin{aligned}{}^{ff'}\rho_Q'^K(t_c^+; b, v_r, \vec{R}_c, t_c)_b = \mathcal{G}(k, k', p, p', K, K', Q; \Delta)\Delta_b^{-2}(-1)^{K + J_{f'} + J_{r'}}[(2J_{r'} + 1)(2k + 1)(2k' + 1)]\delta_{kp}\delta_{k'p'} \\ \times |\langle f'\|\mu'^{(1)}\|r'\rangle|^2 |\langle f\|T^{(k)}\|i\rangle|^2 |\langle r'\|T'^{(k')}\|i'\rangle|^2 \\ \times \begin{Bmatrix} 1 & 1 & K \\ J_{f'} & J_{f'} & J_{r'} \end{Bmatrix}, \end{aligned} \tag{28}$$

where

$$\mathcal{G}(k, k', p, p', K, K', Q; \Delta) = (b\mathcal{E}_c/\hbar w_r)^2 N_I^{-1\,kk'} A_{Q'}^{K'}(b, v_r, 0; \Delta)[{}^{pp'}A_{Q'}^{K'}(b, v_r, 0; \Delta)]^* P_{KQ}. \tag{29}$$

This result is interpreted in terms of Fig. 4(b) as a collisional excitation from ii' to fr' followed by a field exciation of atom A' to the final state ff'.

For the level scheme of Fig. 4(c), one obtains from Eqs. (B3), (B11), and (25c),

$$ {}^{f'f'}\rho'^{K}_{Q}(t_c^+;b,v_r,\vec{R}_c,t_c)_c=\mathcal{C}(k,k',p,p',K,K',Q;\Delta)\Delta_c^{-2}(-1)^{-J_i-J_{i'}-J_{f'}+k+k'+p+p'-2J_r-J_f+K'} $$

$$ \times\left|\langle r\|\mu^{(1)}\|i\rangle\right|^2\langle f\|T^{(k)}\|r\rangle\langle f\|T^{(p)}\|r\rangle^*\langle f'\|T'^{(k')}\|i'\rangle $$

$$ \times\langle f'\|T'^{(p')}\|i'\rangle^*\begin{Bmatrix}1&1&K\\J_r&J_r&J_i\end{Bmatrix}\begin{Bmatrix}k'&p'&K\\J_{f'}&J_{f'}&J_{i'}\end{Bmatrix}\begin{Bmatrix}k&p&K\\p'&k'&K'\end{Bmatrix}\begin{Bmatrix}k&p&K\\J_r&J_r&J_f\end{Bmatrix}. \tag{30} $$

In terms of Fig. 4(c), one interprets this result as a field excitation from ii' to ri' followed by a collisional excitation to ff'.

Finally, for the level scheme of Fig. 4(d), one finds from Eqs. (B3), (B13), and (25d)

$$ {}^{f'f'}\rho'^{K}_{Q}(t_c^+;b,v_r,\vec{R}_c,t_c)_d=\mathcal{C}(k,k',p,p',K,K',Q;\Delta)\Delta_d^{-2}(-1)^{J_{i'}+2J_{r'}+J_{f'}+k'}[(2k+1)(2k'+1)]^{-1} $$

$$ \times\delta_{kp}\delta_{k'p'}\left|\langle r'\|\mu'^{(1)}\|i'\rangle\right|^2\left|\langle f\|T^{(k)}\|i\rangle\right|^2\left|\langle f'\|T'^{(k')}\|r'\rangle\right|^2 $$

$$ \times\begin{Bmatrix}J_{f'}&J_{f'}&K\\J_{r'}&J_{r'}&k'\end{Bmatrix}\begin{Bmatrix}1&1&K\\J_{r'}&J_{r'}&J_{i'}\end{Bmatrix}. \tag{31} $$

In terms of Fig. 4(d), this result corresponds to a field excitation from ii' to ir' followed by a collisional excitation to state ff'.

Equations (26)–(31) characterize the final-state coherence of atom A' for the level schemes of Fig. 4. This coherence can be monitored by measuring the polarization of the fluorescence emitted by atom A' from state f' (see Sec. V).

A. Dipole-dipole interaction

As a somewhat more specific example, I now consider the case where the collisional interaction is of a dipole-dipole nature. For such an interaction, $k=k'=p=p'=1$, $T=\mu$, and $T'=\mu'$. The corresponding ${}^{11}A^{K}_{Q}(b,v_r,0;\Delta)$ are calculated in Appendix C, assuming straight-line collision trajectories.

The results for the dipole-dipole limit are conveniently expressed in terms of the Rabi frequencies

$$ \chi^{c}_{\alpha\beta}=\tfrac{1}{2}\langle\alpha\|\mu^{(1)}\|\beta\rangle\mathcal{E}_c/\hbar, \tag{32a} $$

$$ \chi'^{c}_{\alpha'\beta'}=\tfrac{1}{2}\langle\alpha'\|\mu'^{(1)}\|\beta'\rangle\mathcal{E}_c/\hbar, \tag{32b} $$

and a characteristic length $b^{\alpha'\beta'}_{\alpha\beta}$ defined by

$$ b^{\alpha'\beta'}_{\alpha\beta}=\left|2\langle\alpha\|\mu^{(1)}\|\beta\rangle\langle\alpha'\|\mu'^{(1)}\|\beta'\rangle/\hbar v_r\right|^{1/2}. \tag{33} $$

The quantity $b^{\alpha'\beta'}_{\alpha\beta}$ is a radius that typically appears in theories of resonance broadening ("Weisskopf radius" for resonant broadening) and usually has a value in the 10 to 40 Å range. Moreover, it is useful to define the dimensionless quantity

$$ D_K(\Delta b/v_r)=b^6\sum_Q\left|{}^{11}A^{K}_{Q}(b,v_r,0;\Delta)\right|^2. \tag{34} $$

For the level scheme of Fig. 4(a), the dipole-dipole limit of Eq. (26) is

$$ {}^{f'f'}\rho'^{K}_{Q}(t_c^+;b,v_r,\vec{R}_c,t_c)_a=N_I^{-1}(-1)^{\varphi_a}\left|\chi^{c}_{f_r}/\Delta_a\right|^2(b^{f'i'}_{ri}/b)^4D_{K'}(\Delta b/v_r) $$

$$ \times(-1)^{K'}P_{KQ}\begin{Bmatrix}1&1&K\\J_r&J_r&J_f\end{Bmatrix}\begin{Bmatrix}1&1&K\\J_r&J_r&J_i\end{Bmatrix}\begin{Bmatrix}1&1&K\\1&1&K'\end{Bmatrix}\begin{Bmatrix}1&1&K\\J_{f'}&J_{f'}&J_{i'}\end{Bmatrix}, \tag{35a} $$

where

$$ \varphi_a=J_f-J_{f'}-J_i-J_{i'}. \tag{35b} $$

For the level scheme of Fig. 4(b), the dipole-dipole limit of Eq. (28) is

$$ {}^{f'f'}\rho'^{K}_{Q}(t_c^+;b,v_r,\vec{R}_c,t_c)_b=N_I^{-1}(-1)^{\varphi_b}\left|\chi'^{c}_{f'r'}/\Delta_b\right|^2(b^{r'i'}_{fi}/b)^4[9(2J_{r'}+1)]^{-1} $$

$$ \times D_{K'}(\Delta b/v_r)(-1)^{K}P_{KQ}\begin{Bmatrix}1&1&K\\J_{f'}&J_{f'}&J_{r'}\end{Bmatrix}, \tag{36a} $$

where

$$\varphi_b = J_{f'} + J_{r'} . \tag{36b}$$

For the level scheme of Fig. 4(c), the dipole-dipole limit of Eq. (30) is

$$^{f'f'}\rho_Q'^K(t_c^+; b, v_r, \vec{R}_c, t_c)_c = N_I^{-1}(-1)^{\varphi_c}|\chi_{ri}^c/\Delta_c|^2(b_{fr}^{f'i'}/b)^4 D_{K'}(\Delta b/v_r) \times (-1)^{K'} P_{KQ} \begin{Bmatrix} 1 & 1 & K \\ J_r & J_r & J_i \end{Bmatrix} \begin{Bmatrix} 1 & 1 & K \\ J_{f'} & J_{f'} & J_{i'} \end{Bmatrix} \begin{Bmatrix} 1 & 1 & K \\ 1 & 1 & K' \end{Bmatrix} \begin{Bmatrix} 1 & 1 & K \\ J_r & J_r & J_f \end{Bmatrix}, \tag{37a}$$

where

$$\varphi_c = -J_i - J_{i'} - J_{f'} - 2J_r - J_f . \tag{37b}$$

For the level scheme of Fig. 4(d), the dipole-dipole limit of Eq. (31) is

$$^{f'f'}\rho_Q'^K(t_c^+; b, v_r, \vec{R}_c, t_c)_d = \tfrac{1}{9} N_I^{-1}(-1)^{\varphi_d}|\chi_{r'i'}^c/\Delta_d|^2(b_{fi}^{f'r'}/b)^2 D_{K'}(\Delta b/v_r) \times P_{KQ} \begin{Bmatrix} J_{f'} & J_{f'} & K \\ J_{r'} & J_{r'} & 1 \end{Bmatrix} \begin{Bmatrix} 1 & 1 & K \\ J_{r'} & J_{r'} & J_{i'} \end{Bmatrix}, \tag{38a}$$

where

$$\varphi_d = J_{i'} + 2J_{r'} + J_{f'} + 1 . \tag{38b}$$

Equations (35)–(38) characterize the final-state coherence of atom A' for collisions having impact parameters $b > b_0$, assuming a dipole-dipole collisional interaction.

V. CROSS SECTIONS AND FINAL-STATE COHERENCES FOR A DIPOLE-DIPOLE COLLISIONAL INTERACTION

This section is divided into two parts. In the first part, the RAIC cross sections are calculated for the limiting cases represented in Fig. 4 and discussed in the previous section. In the second part, the polarization of the fluorescence emitted from state f' of atom A' is evaluated.

A. Cross sections

The RAIC cross section is a function of t_c, reflecting the fact that a collision can occur at any time during the on time of the radiation pulse. However, one can define an *average* cross section per pulse for RAIC excitation of $^{f'f_1}\rho_Q'^K(v_r)$ in atom A' as

$$^{f'f_1}\sigma_Q'^K(v_r, \Delta) = \frac{2\pi \int_0^\infty b\, db \int_{T^-}^{T^+} dt_c \int d\vec{R}_c\ {}^{f'f_1}\dot{\rho}_Q'^K(t_c^+; b, v_r, \vec{R}_c, t_c)}{(T^+ - T^-)\int d\vec{R}_c}, \tag{39}$$

where $T^-(T^+)$ represent times just before (after) the radiation pulse and the $\vec{R}_c$ integration is over the atom-field interaction volume. In order to evaluate Eq. (39), an integration over all impact parameters is required. However, the calculation of $^{f'f_1}\rho_Q'^K(t_c^+; b, v_r, \vec{R}_c, t_c)$ presented in Sec. IV is valid only for $b > b_0$, where b_0 is the impact parameter at which the collisional level-shifting operator $\hat{S}_c$ becomes important (see discussion of Sec. II). Thus, some type of cutoff procedure is needed to account for collisions with $b < b_0$.

In this paper, the region $b < b_0$ is treated in an extremely simplified fashion; basically, the contribution from $b < b_0$ is ignored. This overly simplified procedure is, nevertheless, somewhat justified. The parameter b_0 is essentially the Weisskopf radius associated with the level-shifting operator, i.e., that radius at which

$$\varphi_0 = \frac{1}{\hbar}\int_{-\infty}^{\infty} \bar{S}_c(b_0, t)dt = 1 , \tag{40}$$

where $\bar{S}_c$ represents the expectation value of $\hat{S}_c$ in the final-state manifold (typically, $5 < b_0 < 15$ Å). For $b < b_0$ the operator $\hat{S}_c$ strongly couples all final-state magnetic sublevels; it is therefore reasonable to assume that final-state coherences cannot be created for collisions with $b < b_0$. Consequently, the b integral for $\sigma_Q'^K$ $(K > 0)$ can be evaluated from b_0 to ∞. Moreover, collisions with $b < b_0$ can be estimated to contribute less than 20% to the RAIC excitation of final-state *populations*.[8] Thus, the b integral for $\sigma_0'^0$ can also be cut off for $b < b_0$, although the RAIC cross section evaluated in this manner underestimates by 10 to 20% the corresponding cross section calculated without using a cutoff.

In summary, the cutoff procedure adopted is

one in which the lower limit of the b integral in Eq. (39) is replaced by b_0. This procedure underestimates σ'^0_0 by 10 to 20% and provides a good approximation for σ'^K_Q $(K>0)$. The perturbation theory results are valid if ${}^{f'f'}\rho'^0_0(t_c^-, b_0, v_r, \vec{R}_c, t) \ll 1$ (i.e., the final-state population is much less than unity). From Eqs. (32)–(38), and (C14), one can derive the validity condition

$$|\chi^c/\Delta_\alpha|^2(b_R/b_0)^4 \ll 1, \tag{41}$$

where χ^c is a Rabi frequency defined by Eq. (32), b_R is one of the characteristic *resonant* Weisskopf radii defined by Eq. (33), and Δ_α is a frequency mismatch defined by Eq. (25). Since $b_R/b_0 \lesssim 4$ and $|\Delta_\alpha| \gg 10^{12}$ sec^{-1}, Eq. (41) is easily satisfied for a large range of field strengths.

The RAIC excitation cross sections may now be easily obtained for the limiting cases of Fig. 4. For the case of *central tuning*, the RAIC cross section in the dipole-dipole limit for the level scheme corresponding to Fig. 4(a) may be obtained from Eqs. (39), (35a), and (C14) as

$${}^{f'f'}\sigma'^K_Q(v_r, 0)_a = 8\pi N_I^{-1}(-1)^{\varphi_a}(\langle|\chi^c_{f_r}|^2\rangle/\Delta_a^2)(b^{f'i'}_{rf}/b_0)^2(-1)^{Q_s}\epsilon^*_j\epsilon_s \begin{bmatrix} 1 & 1 & K \\ Q_j & -Q_s & Q \end{bmatrix}$$
$$\times \begin{Bmatrix} 1 & 1 & K \\ J_r & J_r & J_f \end{Bmatrix}\begin{Bmatrix} 1 & 1 & K \\ J_r & J_r & J_i \end{Bmatrix}\begin{Bmatrix} 1 & 1 & K \\ 1 & 1 & 2 \end{Bmatrix}\begin{Bmatrix} 1 & 1 & K \\ J_{f'} & J_{f'} & J_{i'} \end{Bmatrix}(b^{f'i'}_{ri})^2, \tag{42}$$

where

$$\langle|\chi^c_{\alpha\beta}|^2\rangle = |\chi^c_{\alpha\beta}|^2\langle\mathcal{E}_c^2\rangle/\mathcal{E}_c^2 \tag{43}$$

and

$$\langle\mathcal{E}_c^2\rangle = \frac{1}{T^+ - T^-}\int d\vec{R}_c \int_{T^-}^{T^+} dt_c |\mathcal{E}_c(\vec{R}_c, t_c)|^2 \Big/ \int d\vec{R}_c. \tag{44}$$

Similarly, for the level scheme of Fig. 4(b), from Eqs. (39), (36a), and (C14) one may obtain

$${}^{f'f'}\sigma'^K_Q(v_r, 0)_b = 8\pi N_I^{-1}(-1)^{\varphi_b}[9(2J_{r'}+1)]^{-1}(\langle|\chi'^c_{f'r'}|^2\rangle/\Delta_b^2)(b^{r'i'}_{fi}/b_0)^2$$
$$\times (-1)^{Q_s}\epsilon^*_j\epsilon_s \begin{bmatrix} 1 & 1 & K \\ Q_j & -Q_s & Q \end{bmatrix}(-1)^K\begin{Bmatrix} 1 & 1 & K \\ J_{f'} & J_{f'} & J_{r'} \end{Bmatrix}(b^{r'i'}_{fi})^2, \tag{45}$$

where

$$\langle|\gamma'^c_{\alpha'\beta'}|^2\rangle = |\chi'^c_{\alpha'\beta'}|^2\langle\mathcal{E}_c^2\rangle/\mathcal{E}_c^2. \tag{46}$$

For the level scheme of Fig. 4(c), the RAIC cross section calculated from Eqs. (39), (37a), and (C14) is

$${}^{f'f'}\sigma'^K_Q(v_r, 0)_c = 8\pi N_I^{-1}(-1)^{\varphi_c}(\langle|\chi^c_{ri}|^2\rangle/\Delta_c^2)(b^{f'i'}_{fr}/b_0)^2(-1)^{Q_s}\epsilon^*_j\epsilon_s$$
$$\times \begin{bmatrix} 1 & 1 & K \\ Q_j & -Q_s & Q \end{bmatrix}\begin{Bmatrix} 1 & 1 & K \\ J_r & J_r & J_i \end{Bmatrix}\begin{Bmatrix} 1 & 1 & K \\ J_{f'} & J_{f'} & J_{i'} \end{Bmatrix}\begin{Bmatrix} 1 & 1 & K \\ 1 & 1 & 2 \end{Bmatrix}\begin{Bmatrix} 1 & 1 & K \\ J_r & J_r & J_f \end{Bmatrix}(b^{f'i'}_{fr})^2. \tag{47}$$

Finally, for the level scheme of Fig. 4(d), one may use Eqs. (39), (38a), and (C14) to obtain

$${}^{f'f'}\sigma'^K_Q(v_r, 0)_d$$
$$= \tfrac{8}{9}\pi N_I^{-1}(-1)^{\varphi_d}(\langle|\chi'^c_{r'i'}|^2\rangle/\Delta_d^2)(b^{f'r'}_{fi}/b_0)^2(-1)^{Q_s}\epsilon^*_j\epsilon_s \begin{bmatrix} 1 & 1 & K \\ Q_j & -Q_s & Q \end{bmatrix}\begin{Bmatrix} J_{f'} & J_{f'} & K \\ J_{r'} & J_{r'} & 1 \end{Bmatrix}\begin{Bmatrix} 1 & 1 & K \\ J_{r'} & J_{r'} & J_{i'} \end{Bmatrix}(b^{f'r'}_{fi})^2. \tag{48}$$

Equations (42), (45), (47), and (48) give the RAIC excitation cross sections for level schemes corresponding to Fig. 4 in the limit of a dipole-dipole collisional interaction. It should be recalled that these are the RAIC cross sections for excitation from an *unpolarized initial state*; the quantities ϵ_j $(j=1, 0, -1)$ specify the polarization of the external field. As defined by Eqs. (33) and (40), the characteristic radii $b^{\alpha'\beta'}_{\alpha\beta}$ and b_0 are functions of v_r; $b^{\alpha'\beta'}_{\alpha\beta}$ is proportional to $v_r^{-1/2}$ and b_0 is proportional to $v_r^{1/(n-1)}$ for a level-shifting operator which varies as R^{-n} $(n>3)$.

The physical significance of the various RAIC cross sections is discussed in Sec. VI. It may be noted at this point, however, that the RAIC cross sections vary as

$$\sigma' = |\Psi(\langle|\chi^c|^2\rangle/\Delta_\alpha^2)(b_R/b_0)^2 b_R^2 , \tag{49}$$

where Ψ is a constant of order unity. Combining Eqs. (41) and (49), one finds that, if the perturbation theory is valid, then

$$\sigma' \ll b_0^2 . \tag{50}$$

Since $b_0 \approx 10$ Å, the maximum RAIC cross sections obtainable with fields satisfying the perturbation-theory requirement (41) are of the order of 100 Å^2. For larger field strengths, where Eq. (41) no longer holds, a strong-field (nonperturbative) theory is needed.

Corresponding results for noncentral tuning ($\Delta \neq 0$) may be obtained from Eqs. (39), (35)–(38), and (C13).

B. Fluorescence

The final-state coherence of atom A' is conveniently monitored by measuring the polarization or quantum beats in the fluorescence emitted from state f'. In this paper, the polarization of the fluorescence is calculated assuming that the external field participating in the RAIC excitation is linearly polarized in the z direction,

$$\epsilon_{\pm 1} = 0, \quad \epsilon_0 = 1 , \tag{51}$$

and propagates in the y direction.

The fluorescence signal emitted from state f' to some lower state g' (characterized by an angular momentum quantum number $J_{g'}$) in atom A' is given by[9]

$$S \propto (-1)^{Q_n} \bar{\epsilon}_i^* \bar{\epsilon}_n (-1)^K \begin{bmatrix} 1 & 1 & K \\ Q_n & -Q_i & Q \end{bmatrix} \times \begin{Bmatrix} 1 & 1 & K \\ J_{f'} & J_{f'} & J_{g'} \end{Bmatrix} \langle {}^{f'f'}\rho_Q'^K(v_r)\rangle , \tag{52}$$

where the $\bar{\epsilon}_i$ ($i = -1, 0, 1$) specify the polarization of the fluorescence according to Eq. (19) (replacing the external-field polarization vector $\vec{\epsilon}$ by the vacuum-field polarization vector $\vec{\bar{\epsilon}}$) and $\langle {}^{f'f'}\rho_Q'^K\rangle$ is the average value of the reduced density-matrix element ${}^{f'f'}\rho_Q'^K$ of atom A'. Adopting a simple model, I assume that the lifetimes of the various ${}^{ff'}\rho_Q'^K$, once created by RAIC, are determined only by the natural decay rate $\gamma_{f'}$ of level f' (i.e., the natural decay rate is much greater than the collision rate and the frequency separation of the final states). In that limit

$$\langle {}^{f'f'}\rho_Q'^K(v_r)\rangle = \mathfrak{N}_A v_r {}^{f'f'}\sigma_Q'^K(v_r) \times [N_p(T^+ - T^-)/\gamma_{f'}] , \tag{53}$$

where $\mathfrak{N}_A$ is the A-atom density and N_p is the number of pulses per second, each of duration $(T^+ - T^-)$. Thus, from Eqs. (52) and (53), one finds

$$S \propto (-1)^{Q_n} \bar{\epsilon}_i^* \bar{\epsilon}_n (-1)^K \begin{bmatrix} 1 & 1 & K \\ Q_n & -Q_i & Q \end{bmatrix} \times \begin{Bmatrix} 1 & 1 & K \\ J_{f'} & J_{f'} & J_{g'} \end{Bmatrix} {}^{f'f'}\sigma_Q'^K(v_r) . \tag{54}$$

For an external field polarized according to (51), it is convenient to measure the fluorescence also propagating in the y direction and polarized in either the x or z direction (Fig. 5). That is, one measures a signal S_x characterized by

$$\bar{\epsilon}_x = 1, \quad \bar{\epsilon}_y = \bar{\epsilon}_z = 0; \quad \bar{\epsilon}_1 = -\bar{\epsilon}_{-1} = \frac{-1}{\sqrt{2}}, \quad \bar{\epsilon}_0 = 0 , \tag{55a}$$

a signal S_z characterized by

$$\bar{\epsilon}_x = \bar{\epsilon}_y = 0, \quad \bar{\epsilon}_z = 1; \quad \bar{\epsilon}_{\pm 1} = 0, \quad \bar{\epsilon}_0 = 1 , \tag{55b}$$

and forms the ratio

$$P = (S_z - S_x)/(S_z + S_x) . \tag{56}$$

Before explicitly calculating this ratio, it is useful to note that the general expression for $\rho_Q'^K$ and, consequently, for $\sigma_Q'^K$ is proportional to

$$P_{KQ} = \epsilon_j^* \epsilon_s (-1)^{Q_s} \begin{bmatrix} 1 & 1 & K \\ Q_j & -Q_s & Q \end{bmatrix}$$

so that, for the excitation scheme of Eq. (51) with the Q_i defined by Eq. (27b), one has

$$P_{KQ} = -(1/\sqrt{3})\,\delta_{K0}\delta_{Q0} + (2/\sqrt{6})\delta_{K2}\delta_{Q0} . \tag{57}$$

Thus only $\sigma_0'^0$ and $\sigma_0'^2$ enter the summation in Eq. (54). Using this fact and Eqs. (54)–(56), one can derive a polarization ratio

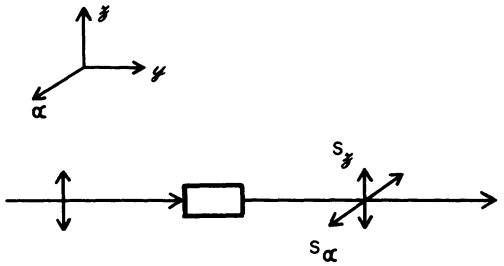

FIG. 5. Excitation-detection scheme. The external field is linearly polarized in the z direction and is incident in the y direction. The fluorescence from the $f' \rightarrow g'$ transition of atom A', propagating in the y direction and polarized in either the x direction (S_x) or z direction (S_z), is monitored.

$$P(\Delta)=3\left(\frac{2\sqrt{6}(-1)^{J_{f'}+J_{g'}}}{3(2J_{f'}+1)^{1/2}}\begin{Bmatrix}1 & 1 & 2\\ J_{f'} & J_f & J_{g'}\end{Bmatrix}^{-1}\frac{f'f'\sigma'^0_0(v_r,\Delta)}{f'f'\sigma'^2_0(v_r,\Delta)}+1\right)^{-1}. \tag{58}$$

Within the confines of the adopted model, the ratio P depends only on *relative* RAIC cross sections and not on *absolute* cross sections. Consequently, it is a useful parameter in comparing theory with experiment.

The ratio P is now calculated for the level schemes of Fig. 4. For the level scheme of Fig. 4(a), it follows from Eqs. (58), (42), and (51) that, for central tuning, $\Delta=0$,

$$P_a(0)=3\left(\frac{20(-1)^{J_f+J_{g'}-J_i-J_{i'}}}{9(2J_{f'}+1)(2J_r+1)\begin{Bmatrix}1 & 1 & 2\\ J_{f'} & J_{f'} & J_{g'}\end{Bmatrix}\begin{Bmatrix}1 & 1 & 2\\ J_{f'} & J_r & J_f\end{Bmatrix}\begin{Bmatrix}1 & 1 & 2\\ J_r & J_r & J_i\end{Bmatrix}\begin{Bmatrix}1 & 1 & 2\\ J_{f'} & J_{f'} & J_{i'}\end{Bmatrix}}+1\right)^{-1}. \tag{59}$$

For the specific case,

$$J_{i'}=J_{g'}=J_i=J_f=0;\quad J_{f'}=J_r=1;\quad P_a(0)=\tfrac{1}{7}, \tag{60}$$

while, for higher J values, $P_a(0)$ is smaller. For the level scheme of Fig. 4(b), one may derive from Eqs. (58), (45), and (51),

$$P_b(0)=3\left(\frac{2(-1)^{J_{r'}-J_{g'}}}{3(2J_{f'}+1)\begin{Bmatrix}1 & 1 & 2\\ J_{f'} & J_{f'} & J_{g'}\end{Bmatrix}\begin{Bmatrix}1 & 1 & 2\\ J_{f'} & J_{f'} & J_{r'}\end{Bmatrix}}+1\right)^{-1}. \tag{61}$$

Some specific cases are

$$J_{g'}=J_{r'}=1,\quad J_{f'}=2,\quad P_b(0)=\tfrac{21}{47}, \tag{62a}$$

$$J_{g'}=J_{r'}=0,\quad J_{f'}=1,\quad P_b(0)=1. \tag{62b}$$

For the level scheme of Fig. 4(c), it follows from Eqs. (58), (47), and (51) that

$$P_c=P_a. \tag{63}$$

This result is unique to the dipole-dipole interaction. For the level scheme of Fig. 4(d), one may derive from Eqs. (58), (48), and (51) that

$$P_d(0)=3\left(\frac{2(-1)^{J_{g'}+J_{i'}}}{3(2J_{f'}+1)(2J_{r'}+1)\begin{Bmatrix}1 & 1 & 2\\ J_{f'} & J_{f'} & J_{g'}\end{Bmatrix}\begin{Bmatrix}J_{f'} & J_{f'} & 2\\ J_{r'} & J_{r'} & 1\end{Bmatrix}\begin{Bmatrix}1 & 1 & 2\\ J_{r'} & J_{r'} & J_{i'}\end{Bmatrix}}+1\right)^{-1}. \tag{64}$$

Some specific cases are

$$J_{i'}=0,\quad J_{g'}=J_{r'}=1,\quad J_{f'}=2,\quad P_d(0)=\tfrac{21}{47}, \tag{65a}$$

$$J_{i'}=J_{f'}=1,\quad J_{g'}=J_{r'}=0,\quad P_d(0)=0. \tag{65b}$$

The physical significance of these results is discussed in the following section.

VI. DISCUSSION

A RAIC is one of the most basic forms of photochemistry. It is, therefore, of fundamental interest to understand the collisional interactions taking part in these reactions. The nature of the collisional interaction is reflected in (1) the total RAIC cross sections, (2) the dependence of RAIC cross sections on detuning Δ, and (3) the final-state coherences produced by RAIC. Total cross-section measurements are not very useful in distinguishing between various collisional interactions since accurate theoretical expressions are not available for comparison with experiment (i.e., there do not exist theoretical calculations in which matrix elements are accurately calculated along with a proper treatment of small-impact-parameter collisions). The dependence of RAIC total cross sections on Δ *does* provide a signature for the collisional interaction, provided one uses de-

tunings outside the impact core of the line $|\Delta|\tau_c > 1$. A limited number of experiments of this type have been performed,[10] but no definite conclusion on the interaction potential was reached. It should be noted that, for $|\Delta|\tau_c > 1$, the RAIC excitation cross sections are relatively small. The study of final-state coherences produced by RAIC offers an additional method for probing the collisional interaction. In many cases (see below), measurements of RAIC-induced final-state coherences at central tuning $\Delta = 0$ (where signal is the largest) are sufficient to provide information concerning the collisional interaction.

Perhaps the most important aspect connected with the study of RAIC-induced coherences is the additional insight one can gain into the RAIC process. The calculation of final-state coherences introduces features into the problem that need not be considered when one calculates *total* RAIC cross sections. A particularly interesting feature can be already seen in the calculation presented in this paper, valid in the impact core of the RAIC profile and in the perturbation-theory limit. The collisional interaction can be viewed as the interaction of two unpolarized multipolar fields with atoms A and A'; the fields are incident from all directions and lead to the simultaneous (virtual) excitation of atoms A and A'. Although the fields are unpolarized, they are, in general, correlated to one another by the coupling coefficients of the collisional interaction [see the discussion of Fig. 4(a) below].

The unpolarized nature of the fields arises from the average over all possible collision orientations. This result may be seen mathematically in Eqs. (A20) and (B2). In Eq. (A20), starting from initial density matrix elements $\rho^{K'}_{Q'}$, one excites final-state density-matrix elements ρ^{K}_{Q} with $|K - K'| \leq 2$. This type of selection rule is precisely that produced by the external field acting alone. In other words, the averaged collisional interaction does not modify the selection rule determined by the external field alone—an average collision acts as a scalar, i.e., as an unpolarized field. Similarly, in Eq. (B2), one sees that, starting from an unpolarized initial state, one excites reduced density-matrix elements ρ'^{K}_{Q} with $K \leq 2$; the selection rule is that associated with the external field only. In contrast to these results, one finds that, for a collision with a *specific* orientation, one could excite density-matrix elements ρ^{K}_{Q} from initial density-matrix elements $\rho^{K'}_{Q'}$ such that $|K - K'| > 2$. It is only the *averaged* collisional interaction that acts as a scalar.

Thus the total RAIC reaction can be viewed as two unpolarized (but correlated) multipolar fields *plus* the external radiation field acting on atoms A and A' to produce the $ii' \rightarrow ff'$ transition. To simulate the collisional interaction, the unpolarized fields are taken to act simultaneously on atoms A and A'; one field acts only on atom A while the other acts only on atom A' (in analogy with the fact that the collision operators act on either atom A or A', but not both). The external field acts on either atom A or A'. Using this model it is relatively easy to give a physical interpretation to the results obtained in Secs. IV and V for the level schemes of Fig. 4.

Figure 4(b). For the level scheme of Fig. 4(b), the collision first acts to produce the virtual state $|fr'\rangle$. If the collision is now replaced by two unpolarized multipolar fields incident from all directions, the coherence properties of this intermediate state are immediately determined. Since the initial state was unpolarized and the average collision operator now acts as a scalar, the intermediate state must also be unpolarized. Thus, when the external field completes the RAIC reaction by acting on atom A', the coherence properties of the final state f' of atom A' are the same as those produced by a radiation field exciting the $r' \rightarrow f'$ transition in atom A' for an initially unpolarized state r'. The factor

$$\epsilon^*_j \epsilon_s (-1)^{Q_s} \begin{bmatrix} 1 & 1 & K \\ Q_j & -Q_s & Q \end{bmatrix} \begin{Bmatrix} 1 & 1 & K \\ J_{f'} & J_{f'} & J_{r'} \end{Bmatrix}$$

appearing in Eq. (45) for the excitation cross section is precisely that associated with the one-photon $r' \rightarrow s'$ transition, assuming state r' to be unpolarized.

The collisional interaction affects the magnitude of the RAIC cross sections through a multiplicative factor. Consequently, the polarization ratio $P_b(0)$ discussed in Sec. V B is independent of the collisional interaction; it depends only on the values $J_{r'}, J_{f'}, J_{g'}$ reflecting the field excitation from $r' \rightarrow f'$ followed by spontaneous emission from f' to g'. Thus, the level scheme [Fig. 4(b)] is not particularly well suited for probing the collisional interaction via polarization studies at line center; RAIC cross sections as a function of frequency are needed.

Figure 4(d). For the level scheme of Fig. 4(d), the field produces a polarized virtual state $|ir'\rangle$ and the two unpolarized fields (collision) complete the transition to state $|ff'\rangle$. The final-state coherence of atom A' can then be thought to be produced by the external field acting on the $i' \rightarrow r'$ transition and an unpolarized multipolar field incident from all directions acting on the transition $r' \rightarrow f'$. The transition amplitude for the $r' \rightarrow f'$ transition depends on the multipolarity of the collision interaction; this dependence is given by the weighting factor

$$\begin{Bmatrix} J_f, & J_{f'}, & K \\ J_r, & J_{r'}, & k' \end{Bmatrix}$$

appearing in Eq. (48). Since this weighting factor couples K and k', the final-state coherence and the polarization ratio P_d can be used to distinguish different collisional interactions.

For the dipole-dipole interaction, $k'=1$, and the collision interaction on atom A' can be replaced by an unpolarized electric field incident from all directions producing the $r' \rightarrow f'$ transition. Thus the coherence properties of state f' of atom A' are the same as those produced by *two-photon excitation* of atom A', the first photon provided by the external field producing the transition $i' \rightarrow r'$ and the second by an unpolarized electric field incident from all directions producing the transition $r' \rightarrow f'$. The polarization ratio $P_d(0)$ for the excitation-detection scheme of Fig. 5 is then easily calculated to be the simple function of $J_{i'}, J_{r'}, J_{f'}, J_{\ell'}$ given by Eq. (64).

Figure 4(a). For the level scheme of Fig. 4(a), the two unpolarized multipolar fields incident from all directions first excite the virtual state $|rf'\rangle$ and the external field acts on atom A to complete the transition to state $|ff'\rangle$. One might think that the final state f' of atom A' would be unpolarized since it was produced by an unpolarized field incident from all directions. However, this conclusion need not be true owing to *correlation* effects between the unpolarized fields. This effect is best illustrated by the case of $J_i = J_f = 0$, $J_r = 1$, and an external field polarized linearly in the z direction. In order for the overall $\Delta m = 0$ selection rule to be satisfied, only that part of the unpolarized field producing a $\Delta m = 0$ transition is utilized. Thus, only a *part* of the unpolarized field acting on atom A is used. Owing to the coupling coefficients $A_{qq'}^{kk'}$ in the collisional interaction, this result implies that, correspondingly, only a *part* of the unpolarized multipolar field acting on atom A' contributes in the $i' \rightarrow f'$ excitation. This result, in turn, implies that state f' can be polarized. For the conditions of Eq. (60), a polarization ratio $P_a(0) = \frac{1}{7}$ was found. Since the polarization ratio for case Fig. 4(a) is a function of the multipolarity of the collisional interaction, it can be used to provide an indication of the collisional processes participating in RAIC.

Figure 4(c). The analysis of the level scheme of Fig. 4(c) is similar to that for Fig. 4(a), except that the field acts on atom A' rather than on atom A. For the dipole-dipole interaction, in which the external field and the collisional operators have the same multipolarity ($k = k' = p = p' = 1$), the RAIC cross sections for cases Figs. 4(a) and 4(d) are proportional to one another; for other collisional interactions, this proportionality is lost.

In order to have a more complete picture of the final-state coherences produced by RAIC, it is desirable to extend the theory to include the cases of large detuning ($|\Delta|\tau_c > 1$) and large field strengths (nonperturbative solution). Such extensions may pose some interesting problems in the average over collision orientations, since the collision interaction no longer enters linearly in the final-state amplitude. Owing to this nonlinearity, the analog between an average collision and an unpolarized field may no longer be useful.

In summary, I have presented a calculation of the final-state coherences produced by RAIC in the weak-field limit that is valid in the impact core of the RAIC excitation profile. The resulting final-state coherences can be monitored by standard techniques (polarization of fluorescence, quantum beats) and may provide information on the collisional interactions occurring in the RAIC reaction.

ACKNOWLEDGMENT

This research was carried out while I was a guest at the Laboratoire Aimé Cotton, Orsay, France. The hospitality shown to me during my stay is deeply acknowledged as are conversations with C. Bréchignac, Ph. Cahuzac, J. L. Le Gouët, J. L. Picqué, and R. Vetter. I should also like to acknowledge financial support from the Fulbright Foundation. This research was also supported by the U. S. Office of Naval Research.

APPENDIX A

Appendix A is divided into three parts. In part A, some notation is introduced and the relationship between the direct product and irreducible-tensor subspaces is established. In part B, the relationship between the two-particle and single-particle (reduced) density-matrix elements is given. Finally, in part C, the final-state density-matrix for RAIC is calculated.

A. Relationship between bases

A state of the composite AA' system is represented by a capital letter, e.g.,

$$|F\rangle = |ff'\rangle = |f\rangle\,|f'\rangle' \equiv |fJ_f m_f\rangle\,|f'J_{f'} m_{f'}\rangle', \tag{A1}$$

where it has been assumed that the angular momentum of a level can be represented by a J quantum number. The angular momenta appearing in the direct product basis (A1) can be coupled in the standard fashion,

$$|\bar{F}\rangle \equiv |ff'J_fJ_{f'}J_F m_F\rangle$$

$$= \begin{bmatrix} J_f & J_{f'} & J_F \\ m_f & m_{f'} & m_F \end{bmatrix} |fJ_f m_f\rangle |f'J_{f'} m_{f'}\rangle', \quad \text{(A2)}$$

where the bar indicates this coupled basis. As in the main text, I use a summation convention in which all repeated indices (not including their appearance in phase factors or frequency denominators) are summed over.[2]

Matrix elements of the density-matrix operator in the barred basis are related to those in an irreducible tensor basis, ${}^{\bar{F}\bar{F}_1}\rho_Q^K$, via the transformations

$$\rho_{\bar{F}\bar{F}_1} = \langle \bar{F}|\rho|\bar{F}_1\rangle = (-1)^{J_{\bar{F}_1} - m_{\bar{F}_1}} \begin{bmatrix} J_{\bar{F}} & J_{\bar{F}_1} & K \\ m_{\bar{F}} & -m_{\bar{F}_1} & Q \end{bmatrix} {}^{\bar{F}\bar{F}_1}\rho_Q^K , \quad \text{(A3a)}$$

$${}^{\bar{F}\bar{F}_1}\rho_Q^K = (-1)^{J_{\bar{F}_1} - m_{\bar{F}_1}} \begin{bmatrix} J_{\bar{F}} & J_{\bar{F}_1} & K \\ m_{\bar{F}} & -m_{\bar{F}_1} & Q \end{bmatrix} \times \langle \bar{F} J_{\bar{F}} m_{\bar{F}} | \rho | \bar{F}_1 J_{\bar{F}_1} m_{\bar{F}_1} \rangle , \quad \text{(A3b)}$$

where the total J and m_J values of the barred basis are explicitly written in the right-hand side of Eq. (A3b).

The time rate of change of density-matrix elements produced by RAIC can be expressed as[4]

$$\dot{\rho}_{FF_1} = \Gamma^{II_1}_{FF_1} \rho_{II_1} \quad \text{(A4a)}$$

or

$${}^{\bar{F}\bar{F}_1}\dot{\rho}_Q^K = \Gamma^{K'Q'}_{KQ}(\bar{F}, \bar{F}_1, \bar{I}, \bar{I}_1)\, {}^{\bar{I}\bar{I}_1}\rho_{Q'}^{K'} . \quad \text{(A4b)}$$

The relationship between the Γ's may be obtained from Eqs. (A1)–(A4) as

$$\Gamma^{K'Q'}_{KQ}(\bar{F}, \bar{F}_1, \bar{I}, \bar{I}_1) = (-1)^{\bar{I}_1 - m_{\bar{I}_1}} (-1)^{\bar{F}_1 - m_{\bar{F}_1}} \begin{bmatrix} J_f & J_{f'} & J_{\bar{F}} \\ m_f & m_{f'} & m_{\bar{F}} \end{bmatrix} \begin{bmatrix} J_{f_1} & J_{f_1'} & J_{\bar{F}_1} \\ m_{f_1} & m_{f_1'} & m_{\bar{F}_1} \end{bmatrix}$$

$$\times \begin{bmatrix} J_{\bar{F}} & J_{\bar{F}_1} & K \\ m_{\bar{F}} & -m_{\bar{F}_1} & Q \end{bmatrix} \begin{bmatrix} J_i & J_{i'} & J_{\bar{I}} \\ m_i & m_{i'} & m_{\bar{I}} \end{bmatrix} \begin{bmatrix} J_{i_1} & J_{i_1'} & J_{\bar{I}_1} \\ m_{i_1} & m_{i_1'} & m_{\bar{I}_1} \end{bmatrix} \begin{bmatrix} J_{\bar{I}} & J_{\bar{I}_1} & K' \\ m_{\bar{I}} & -m_{\bar{I}_1} & Q' \end{bmatrix}$$

$$\times \Gamma^{II_1}_{FF_1}(m_f, m_{f'}, m_{f_1}, m_{f_1'}, m_{i'}, m_{i_1}, m_{i_1'}) \quad \text{(A5)}$$

along with the corresponding inverse transformation.

B. Reduced density-matrix elements

The reduced density-matrix elements for atom A' are defined by

$$\rho'_{f'f_1'} = \langle ff'|\rho|ff_1'\rangle . \quad \text{(A6)}$$

In terms of the matrix elements of irreducible-tensor operators defined by Eq. (23a), one can use Eqs. (A1)–(A3) and some elementary properties of the Clebsch-Gordon coefficient to derive

$${}^{f'f_1'}\rho'^K_Q = (-1)^{J_{f_1'} + J_{\bar{F}} + J_f - K} [(2J_{\bar{F}}+1)(2J_{\bar{F}_1}+1)]^{1/2} \begin{Bmatrix} J_{\bar{F}} & J_{\bar{F}_1} & K \\ J_{f_1'} & J_{f_1} & J_f \end{Bmatrix} {}^{\bar{F}\bar{F}_1}\rho_Q^K (ff'J_fJ_{f'}J_{\bar{F}}; ff_1'J_fJ_{f_1'}J_{\bar{F}_1}) . \quad \text{(A7)}$$

Equation (A7), in which the $\{\ \}$ represents a 6-J symbol, enables one to calculate the reduced density-matrix elements of atom A' from the two-particle density-matrix elements. Similarly, reduced matrix elements of atom A are given by

$$\rho_{ff_1} = \langle ff'|\rho|f_1f'\rangle \quad \text{(A8)}$$

and

$${}^{ff_1}\rho_Q^K = (-1)^{J_f + J_{\bar{F}_1} + J_{f'} - K} [(2J_{\bar{F}}+1)(2J_{\bar{F}_1}+1)]^{1/2} \begin{Bmatrix} J_{\bar{F}} & J_{\bar{F}_1} & K \\ J_{f_1} & J_f & J_{f'} \end{Bmatrix} {}^{\bar{F}\bar{F}_1}\rho_Q^K (ff'J_fJ_{f'}J_{\bar{F}}; f_1f'J_{f_1}J_{f'}J_{\bar{F}_1}) . \quad \text{(A9)}$$

C. Calculation of $^{\overline{FF}_1}\rho^K_Q$

Starting from Eq. (10), I now derive an expression for $^{\overline{FF}_1}\rho^K_Q(t_c^+; b, v_r, \vec{R}_c, t_c)$. Equation (10) may be written

$$a_F(t_c^+) = \langle F | \tilde{T} | I \rangle a_I(t_c^-) , \tag{A10a}$$

where

$$\langle F | \tilde{T} | I \rangle = (i\hbar)^{-1} \int_{t_c^-}^{t_c^+} \langle F | \hat{T}(IF, t) | I \rangle e^{-i\Delta t} dt . \tag{A10b}$$

Equation (A10a) could equally well be given in the coupled (barred) basis as

$$a_{\overline{F}}(t_c^+) = \langle \overline{F} | \tilde{T} | \overline{I} \rangle a_{\overline{I}}(t_c^-) , \tag{A11}$$

so that the final-state density matrix is

$$\rho_{\overline{F}\overline{F}_1}(t_c^+; b, v_r, \Theta, \vec{R}_c, t_c) = \langle \overline{F} | \tilde{T} | \overline{I} \rangle \langle \overline{F}_1 | \tilde{T} | \overline{I}_1 \rangle^* \rho_{\overline{I}\overline{I}_1}(t_c^-) . \tag{A12}$$

The matrix elements of $\tilde{T}$ are expanded as

$$\langle \overline{F} | \tilde{T} | \overline{I} \rangle = (-1)^{J_{\overline{I}} - m_{\overline{I}}} \begin{bmatrix} J_{\overline{F}} & J_{\overline{I}} & G \\ m_{\overline{F}} & -m_{\overline{I}} & g \end{bmatrix} {}^{\overline{F}\overline{I}}\tilde{T}^G_g . \tag{A13}$$

Equation (A3a) is used, and some identities involving the angular momentum coupling coefficients are employed to transform equation (A12) into

$$^{\overline{FF}_1}\rho^K_Q(t_c^+; b, v_r, \vec{R}_c, t_c) = (-1)^{2J_{\overline{F}} + G' + 2J_{\overline{I}} + K'} (-1)^{g'+Q'} [(2G+1)(2G'+1)(2K+1)(2K'+1)]^{1/2}$$

$$\times \begin{bmatrix} K & K' & X \\ Q & -Q' & m_x \end{bmatrix} \begin{bmatrix} G & G' & X \\ g & -g' & m_x \end{bmatrix} \begin{Bmatrix} \overline{F} & \overline{F}_1 & K \\ \overline{I} & \overline{I}_1 & K' \\ G & G' & X \end{Bmatrix} H(\overline{F}, \overline{F}_1, \overline{I}, \overline{I}_1, G, G', g, g') {}^{\overline{II}_1}\rho^{K'}_{Q'}(t_c^-) , \tag{A14}$$

where

$$H(\overline{F}, \overline{F}_1, \overline{I}, \overline{I}_1, G, G', g, g') \equiv (8\pi^2)^{-1} \int d\Theta \, {}^{\overline{FI}}\tilde{T}^G_g ({}^{\overline{F}_1\overline{I}_1}\tilde{T}^{G'}_{g'})^* \tag{A15}$$

and the quantity in large curly brackets is a 9-J symbol. The quantities ${}^{\overline{FI}}\tilde{T}^G_g$ may be calculated by (i) using Eqs. (A13), (A10b), (6), (13), (18); (ii) expanding all intermediate states appearing in Eq. (6) in terms of the barred basis; and (iii) using the Wigner-Eckart theorem to evaluate matrix elements of $(\mu_T)^1_q$ and $^{kk'}V^K_Q$. One obtains

$$\begin{aligned} {}^{\overline{FI}}\tilde{T}^G_g = {} & (-1)^{3J_{\overline{F}} + J_{\overline{I}} + 2J_{\overline{E}} + K + 1} \langle \overline{F} \| (\mu_T)^{(1)} \| \overline{E} \rangle \langle \overline{E} \| {}^{kk'}V^{(K)} \| \overline{I} \rangle (\omega_{EI})^{-1} \\ & \times (i\hbar)^{-1} \left(\frac{b}{v_r} \right) {}^{kk'}A^K_Q(b, v_r, \Theta; \Delta) \epsilon^*_j \begin{bmatrix} K & 1 & G \\ Q & Q_j & g \end{bmatrix} \begin{Bmatrix} K & 1 & G \\ J_{\overline{I}} & J_{\overline{F}} & J_{\overline{E}} \end{Bmatrix} \mathcal{S}_c \\ & + (-1)^{J_{\overline{F}} + J_{\overline{I}} + G} \langle \overline{F} \| {}^{kk'}V^{(K)} \| \overline{E} \rangle \langle \overline{E} \| (\mu_T)^{(1)} \| \overline{I} \rangle (\omega_{EF})^{-1} \\ & \times (i\hbar)^{-1} \left(\frac{b}{v_r} \right) {}^{kk'}A^K_Q(b, v_r, \Theta; \Delta) \epsilon^*_j \begin{bmatrix} K & 1 & G \\ Q & Q_j & g \end{bmatrix} \begin{Bmatrix} K & 1 & G \\ J_{\overline{I}} & J_{\overline{F}} & J_{\overline{E}} \end{Bmatrix} \mathcal{S}_c \end{aligned} \tag{A16}$$

where $^{kk'}A^K_Q(b, v_r, \Theta; \Delta)$ is defined by Eq. (16b), $\langle \| \cdots \| \rangle$ is a reduced matrix element, ϵ_j is defined by Eqs. (17)–(19), and

$$Q_1=1,\ Q_{-1}=-1,\ Q_0=0. \tag{A17}$$

Equation (A16) and its complex conjugate are now inserted into Eq. (A15), and Eqs. (15) and (21) are used to arrive at

$$H(\bar{F},\bar{F}_1,\bar{I},\bar{I}_1,\ G,G',g,g')=\left(\frac{b\mathcal{E}_c}{\hbar v_r}\right)^2(2K+1)^{-1}\epsilon_j^*\epsilon_s\,{}^{kk'}A_Q^K(b,v_r,0;\Delta)[{}^{pp'}A_Q^K(b,v_r,0;\Delta)]^*$$
$$\times\begin{bmatrix}K & 1 & G\\ Q & Q_j & g\end{bmatrix}\begin{bmatrix}K & 1 & G'\\ Q' & Q_s & g'\end{bmatrix}C(\bar{F},\bar{I},G,k,k',K)[C(\bar{F}_1,\bar{I}_1,G',p,p',K)]^*, \tag{A18}$$

where

$$C(\bar{F},\bar{I},G,k,k',K)=(-1)^{3J_{\bar{F}}+J_{\bar{I}}+2J_{\bar{E}}+K+1}(\omega_{EI})^{-1}\langle\bar{F}||(\mu_T)^{(1)}||\bar{E}\rangle\langle\bar{E}||{}^{kk'}V^{(K)}||\bar{I}\rangle\begin{Bmatrix}K & 1 & G\\ J_{\bar{F}} & J_{\bar{I}} & J_{\bar{E}}\end{Bmatrix}$$
$$+(-1)^{J_{\bar{F}}+J_{\bar{I}}+G}(\omega_{EF})^{-1}\langle\bar{F}||{}^{kk'}V^{(K)}||\bar{E}\rangle\langle\bar{E}||(\mu_T)^{(1)}||\bar{I}\rangle\begin{Bmatrix}K & 1 & G\\ J_{\bar{I}} & J_{\bar{F}} & J_{\bar{E}}\end{Bmatrix}. \tag{A19}$$

The quantity C is easily identified with the four diagrams of Figs. 2 and 3.

Combining Eqs. (A18) and (A19) and carrying out the summations over magnetic quantum numbers, one obtains

$${}^{\bar{F}\bar{F}_1}\rho_Q^K(t_c^+;b,v_r,\vec{R}_c,t_c)=(-1)^{2J_{\bar{I}}+2J_{\bar{F}}+G+K'+\bar{F}+X}(-1)^{Q'+Q_j+m_x}\left(\frac{b\mathcal{E}_c}{\hbar v_r}\right)^2$$
$$\times\epsilon_j^*\epsilon_s[(2G+1)(2G'+1)(2K+1)(2K'+1)]^{1/2}\begin{bmatrix}K & K' & X\\ Q & -Q' & m_x\end{bmatrix}$$
$$\times\begin{bmatrix}1 & 1 & X\\ Q_j & -Q_s & m_x\end{bmatrix}{}^{kk'}A_{\tilde{Q}}^{\tilde{K}}(b,v_r,0;\Delta)[{}^{pp'}A_{\tilde{Q}}^{\tilde{K}}(b,v_r,0;\Delta)]^*\begin{Bmatrix}1 & 1 & X\\ G & G' & \tilde{K}\end{Bmatrix}\begin{Bmatrix}\bar{F} & \bar{F}_1 & K\\ \bar{I} & \bar{I}_1 & K'\\ G & G' & X\end{Bmatrix}$$
$$\times C(\bar{F},\bar{I},G,k,k',\tilde{K})[C(\bar{F}_1,\bar{I}_1,G',p,p',\tilde{K})]^*{}^{\bar{I}\bar{I}_1}\rho_{Q'}^{K'}(t_c^-). \tag{A20}$$

It is clear from this equation that $|K'-K|<2$, i.e., that the collision acts in some way as a scalar operator (see Sec. VI). Reduced density-matrix elements may be obtained from Eq. (A20) by use of Eqs. (A7) and (A9). Density-matrix elements in the magnetic sublevel basis are related to those in the irreducible tensor basis by Eqs. (A3) and (A2) or, for reduced density-matrix elements, by Eq. (23b).

APPENDIX B

Unpolarized initial state

In Appendix B, the reduced density-matrix elements for atom A' are calculated *for an unpolarized initial state.* An unpolarized initial state corresponds to

$${}^{\bar{I}\bar{I}_1}\rho_Q^K(t_c^-)=(2J_{\bar{I}}+1)^{1/2}N_I^{-1}\delta_{\bar{I}\bar{I}_1}\delta_{K0}\delta_{Q0}, \tag{B1}$$

where N_I is the total number of initial states. Using Eqs. (A7), (A20), and (B1), one may obtain after a little algebra[5] the reduced density-matrix elements for atom A',

$${}^{f'f_1'}\rho_Q'^K(t_c^+;b,v_r,\vec{R}_c,t_c)=\sum_f(-1)^{J_f+J_{f_1'}+K+K'+G+G'}\left(\frac{b\mathcal{E}_c}{\hbar v_r}\right)^2(2G+1)(2G'+1)$$
$$\times[(2J_{\bar{F}}+1)(2J_{\bar{F}_1}+1)]^{1/2}[N_I(2K'+1)]^{-1}{}^{kk'}A_{Q'}^{K'}(b,v_r,0;\Delta)$$
$$\times{}^{pp'}A_{Q'}^{K'}(b,v_r,0;\Delta)]^*\epsilon_j^*\epsilon_s(-1)^{Q_s}\begin{bmatrix}1 & 1 & K\\ Q_j & -Q_s & Q\end{bmatrix}\begin{Bmatrix}1 & 1 & K\\ G & G' & K'\end{Bmatrix}$$
$$\times\begin{Bmatrix}G & G' & K\\ J_{\bar{F}_1} & J_{\bar{F}} & J_{\bar{I}}\end{Bmatrix}\begin{Bmatrix}J_{\bar{F}_1} & J_{\bar{F}} & K\\ J_{f'} & J_{f_1'} & J_f\end{Bmatrix}C(\bar{F},\bar{I},G,k,k',K')$$
$$\times[C(\bar{F}_1,\bar{I},G',p,p',K')]^*. \tag{B2}$$

The product of the C's can be calculated explicitly and the final expression simplified using identities involving the angular momenta coupling coefficients.[5]

One obtains 16 terms corresponding to the square of the four terms contributing to the amplitude in Fig. 2. The result may be written in the form

$$f'f'_1\rho'^{K}_{Q}(t_c^+;b,v_r,\vec{R}_c,t_c)=\left(\frac{b\mathcal{E}_c}{\hbar v_r}\right)^2 N_I^{1kk'}A^{K'}_{Q'}(b,v_r,0;\Delta)[^{pp'}A^{K'}_{Q'}(b,v_r,0;\Delta)]^*\epsilon^*_f\epsilon_a(-1)^{Q_a}\begin{bmatrix}1 & 1 & K\\ Q_f & -Q_a & Q\end{bmatrix}$$

$$\times\sum_{\alpha,\beta=a}^{d}\mathcal{G}_{\alpha\beta}(k,k',p,p',K,K',f',f'_1)\,, \tag{B3}$$

where $\mathcal{G}_{\alpha\beta}$ represents the contribution from diagram α and the complex conjugate of diagram β in Fig. 2. Explicitly,

$$\mathcal{G}_{aa}=[(\omega_e+\omega_{f'}-\omega_I)(\omega_d+\omega_{f'}-\omega_I)]^{-1}(-1)^{J_e-J_d-J_{f'}+J_f-J_i-J_{i'}+K'+p'+k'}$$
$$\times\langle f\,||\mu^{(1)}||e\rangle\langle f\,||\mu^{(1)}||d\rangle^*\langle e||T^{(k)}||i\rangle\langle d||T^{(p)}||i\rangle^*\langle f'||T'^{(k')}||i'\rangle\langle f'_1||T'^{(p')}||i'\rangle^*$$
$$\times\begin{Bmatrix}1 & 1 & K\\ J_e & J_d & J_f\end{Bmatrix}\begin{Bmatrix}k & p & K\\ J_d & J_e & J_i\end{Bmatrix}\begin{Bmatrix}k' & p' & K\\ p & k & K'\end{Bmatrix}\begin{Bmatrix}k' & p' & K\\ J_{f'_1} & J_{f'} & J_{i'}\end{Bmatrix}, \tag{B4}$$

$$\mathcal{G}_{ab}=[(\omega_e+\omega_{f'}-\omega_I)(\omega_f+\omega_{d'}-\omega_I)]^{-1}(-1)^{K-2J_e+J_{d'}+J_f-J_i-J_{i'}+k'+p'}$$
$$\times\langle f\,||\mu^{(1)}||e\rangle\langle f'_1||\mu'^{(1)}||d'\rangle^*\langle e||T^{(k)}||i\rangle\langle f\,||T^{(p)}||i\rangle^*\langle f'||T'^{(k')}||i'\rangle\langle f'_1||T'^{(p')}||d'\rangle^*$$
$$\times\begin{Bmatrix}1 & 1 & K\\ J_{f'} & J_{f'_1} & J_{d'}\end{Bmatrix}\begin{Bmatrix}k & p & 1\\ k' & p' & K'\end{Bmatrix}\begin{Bmatrix}k & p & K'\\ J_f & J_e & J_i\end{Bmatrix}\begin{Bmatrix}k' & p' & 1\\ J_{d'} & J_{f'} & J_{i'}\end{Bmatrix}, \tag{B5}$$

$$\mathcal{G}_{bb}=[(\omega_f+\omega_{e'}-\omega_I)(\omega_F+\omega_{d'}-\omega_I)]^{-1}(-1)^{K+J_{f'}+J_{e'}}[(2J_{e'}+1)(2k+1)(2k'+1)]^{-1}$$
$$\times\delta_{J_{e'}J_{d'}}\delta_{kp}\delta_{k'p'}\langle f'||\mu'^{(1)}||e'\rangle\langle f'_1||\mu'^{(1)}||d'\rangle^*|\langle F||T^{(k)}||i\rangle|^2\langle e'||T'^{(k')}||i'\rangle$$
$$\times\langle d'||T'^{(k')}||i'\rangle^*\begin{Bmatrix}1 & 1 & K\\ J_{f'} & J_{f'_1} & J_{e'}\end{Bmatrix}, \tag{B6}$$

$$\mathcal{G}_{ac}=[(\omega_e+\omega_{f'}-\omega_I)(\omega_d+\omega_{i'}-\omega_F)]^{-1}(-1)^{J_i+J_{i'}+J_d-J_e+K'+K+J_{f'}+k'+p+p'+J_{f'_1}}$$
$$\times\langle f||\mu^{(1)}||e\rangle\langle d||\mu^{(1)}||i\rangle^*\langle e||T^{(k)}||i\rangle\langle f||T^{(p)}||d\rangle^*\langle f'||T'^{(k')}||i'\rangle\langle f'_1||T'^{(p')}||i'\rangle^*$$
$$\times\begin{Bmatrix}k' & p' & K\\ p & k & K'\end{Bmatrix}\begin{Bmatrix}k' & p' & K\\ J_{f'_1} & J_{f'} & J_{i'}\end{Bmatrix}\begin{Bmatrix}1 & 1 & K\\ J_d & J_f & p\\ J_i & J_e & k\end{Bmatrix}, \tag{B7}$$

$$\mathcal{G}_{ad}=[(\omega_e+\omega_{f'}-\omega_I)(\omega_i+\omega_{d'}-\omega_F)]^{-1}(-1)^{J_i+J_{i'}+J_{d'}+J_{f'}+2J_f+k'+J_e+K}$$
$$\times\langle f\,||\mu^{(1)}||e\rangle\langle d'||\mu'^{(1)}||i'\rangle^*\langle e||T^{(k)}||i\rangle\langle f\,||T^{(p)}||i\rangle^*\langle f'||T'^{(k')}||i'\rangle$$
$$\times\langle f'_1||T'^{(p')}||d'\rangle^*$$
$$\times\begin{Bmatrix}k & p & 1\\ p' & k' & K'\end{Bmatrix}\begin{Bmatrix}k & p & 1\\ J_f & J_e & J_i\end{Bmatrix}\begin{Bmatrix}1 & K & 1\\ J_{d'} & J_{f'_1} & p'\\ J_{i'} & J_{f'} & k'\end{Bmatrix}, \tag{B8}$$

$$\mathcal{G}_{bc}=[(\omega_f+\omega_{e'}-\omega_I)(\omega_d+\omega_{i'}-\omega_F)]^{-1}(-1)^{J_{i'}-J_i+1-J_{f'}+K-J_f+J_{f'_1}+K'-J_{e'}+k+k'+p+p'}$$
$$\times\langle f'||\mu'^{(1)}||e'\rangle\langle d||\mu^{(1)}||i\rangle^*\langle f\,||T^{(k)}||i\rangle\langle f||T^{(p)}||d\rangle^*\langle e'||T'^{(k')}||i'\rangle$$
$$\times\langle f'_1||T'^{(p')}||i'\rangle^*$$
$$\times\begin{Bmatrix}1 & 1 & K\\ J_{f'} & J_{f'_1} & J_{e'}\end{Bmatrix}\begin{Bmatrix}k & p & 1\\ J_d & J_i & J_f\end{Bmatrix}\begin{Bmatrix}k' & p' & 1\\ p & k & K'\end{Bmatrix}\begin{Bmatrix}k' & p' & 1\\ J_{f'_1} & J_{e'} & J_{i'}\end{Bmatrix}, \tag{B9}$$

$$\mathcal{G}_{bd} = [(\omega_f + \omega_{e'} - \omega_I)(\omega_i + \omega_{d'} - \omega_F)]^{-1}(-1)^{2J_i+1-J_{f'}-J_f+K'+J_{d'}+k'}$$
$$\times [(2k+1)(2k'+1)]^{-1}\delta_{pk}\delta_{p'k'}\langle f' || \mu'^{(1)} || e'\rangle\langle d' || \mu'^{(1)} || i'\rangle^*$$
$$\times |\langle f || T^{(k)} || i\rangle|^2 \langle e' || T'^{(k')} || i'\rangle\langle f_1' || T'^{(k')} || d'\rangle^* \begin{Bmatrix} 1 & 1 & K \\ J_{f'} & J_{f_1'} & J_{e'} \end{Bmatrix} \begin{Bmatrix} J_{f_1'} & J_{d'} & k' \\ J_{i'} & J_{e'} & 1 \end{Bmatrix}, \tag{B10}$$

$$\mathcal{G}_{cc} = [(\omega_e + \omega_{i'} - \omega_F)(\omega_d + \omega_{i'} - \omega_F)]^{-1}(-1)^{-J_i-J_{i'}-J_{f'}+k+k'+p+p'-J_d-J_e-J_f+K'}$$
$$\times \langle e || \mu^{(1)} || i\rangle\langle d || \mu^{(1)} || i\rangle^* \langle f || T^{(k)} || e\rangle\langle f' || T'^{(k')} || i'\rangle\langle f_1' || T'^{(p')} || i'\rangle^*$$
$$\times \begin{Bmatrix} 1 & 1 & K \\ J_e & J_d & J_i \end{Bmatrix} \begin{Bmatrix} k' & p' & K \\ J_{f_1'} & J_{f'} & J_{i'} \end{Bmatrix} \begin{Bmatrix} k & p & K \\ p' & k' & K' \end{Bmatrix} \begin{Bmatrix} k & p & K \\ J_d & J_e & J_f \end{Bmatrix}, \tag{B11}$$

$$\mathcal{G}_{cd} = [(\omega_e + \omega_{i'} - \omega_F)(\omega_i + \omega_{d'} - \omega_F)]^{-1}(-1)^{J_i+J_{i'}+J_{d'}+K+K'+p+k+k'+J_f+2J_{f'}}$$
$$\times \langle e \| \mu^{(1)} \| i\rangle\langle d' \| \mu'^{(1)} \| i'\rangle^* \langle f \| T^{(k)} \| e\rangle\langle f \| T^{(p)} \| i\rangle^* \langle f' \| T'^{(k')} \| i'\rangle\langle f_1' \| T'^{(p')} \| d'\rangle^*$$
$$\times \begin{Bmatrix} k & p & 1 \\ p' & k' & K' \end{Bmatrix} \begin{Bmatrix} k & p & 1 \\ J_i & J_e & J_f \end{Bmatrix} \begin{Bmatrix} J_{f_1'} & K & J_{f'} \\ J_{d'} & 1 & J_{i'} \\ p' & 1 & k' \end{Bmatrix}, \tag{B12}$$

$$\mathcal{G}_{dd} = [(\omega_i + \omega_{e'} - \omega_F)(\omega_i + \omega_{d'} - \omega_F)]^{-1}(-1)^{J_{i'}+2J_{e'}+J_{f_1'}+k'}[(2k+1)(2k'+1)]^{-1}$$
$$\times \delta_{kp}\delta_{k'p'}\langle e' \| \mu'^{(1)} \| i'\rangle\langle d' \| \mu'^{(1)} \| i'\rangle^* |\langle f \| T^{(k)} \| i\rangle|^2 \langle f' \| T'^{(k')} \| e'\rangle$$
$$\times \langle f_1' \| T'^{(k')} \| d'\rangle^* \begin{Bmatrix} J_{f_1'} & J_{f'} & K \\ J_{e'} & J_{d'} & k' \end{Bmatrix} \begin{Bmatrix} 1 & 1 & K \\ J_{e'} & J_{d'} & J_{i'} \end{Bmatrix}, \tag{B13}$$

and

$$\mathcal{G}_{\alpha\beta}(k,k',p,p',K,K',f',f_1') = (-1)^{J_{f_1'}-J_{f'}}[\mathcal{G}_{\beta\alpha}(p,p',k,k',K,K',f_1',f')]^* . \tag{B14}$$

Some of these terms may vanish owing to the selection rules appropriate to the level-coupling scheme and interatomic potential under consideration.

APPENDIX C

Dipole-dipole interaction

In Appendix C, the quantities $A_{qq'}^{kk'}$ and ${}^{kk'}A_Q^K$ are evaluated, assuming a dipole-dipole collisional interaction between atom A (dipole-moment operator $\vec{\mu}$) and atom A' (dipole-moment operator $\vec{\mu}'$) of the form

$$\mathcal{U} = (\vec{\mu}\cdot\vec{\mu}' R^2 - 3\vec{\mu}\cdot\vec{R}\,\vec{\mu}'\cdot\vec{R})/R^5 , \tag{C1}$$

where $\vec{R}$ is the separation between the atoms. For a given collision geometry, $\vec{R}$ is a function of $\tau = t - t_c$ (the collision is centered in time at $t = t_c$), b, v_r, and Θ.

Writing $\vec{\mu}$ and $\vec{\mu}'$ in the form of Eq. (20) and defining

$$R_1 = -\frac{(R_x - iR_y)}{\sqrt{2}}, \quad R_{-1} = \frac{R_x + iR_y}{\sqrt{2}}, \quad R_0 = R_z , \tag{C2}$$

one may rewrite Eq. (C1) as

$$\mathcal{U} = A_{qq'}^{11}(\tau, b, v_r, \Theta)\mu_q^1(\mu')_{q'}^1 , \tag{C3}$$

where

$$A^{11}_{qq'}(\tau, b, v_r, \Theta) = [R^2(\delta_{q0}\delta_{q'0} - \delta_{q1}\delta_{q',-1} - \delta_{q,-1}\delta_{q'1}) - 3R_qR_{q'}]/R^5 . \tag{C4}$$

Equation (C3) has exactly the same form as Eq. (12) since μ^1_q and $(\mu')^1_q$ are components of irreducible tensors of rank 1.

The quantities of interest in evaluating RAIC cross sections are the Fourier transform of the $A^{11}_{qq'}$ defined by Eq. (16a). Using Eqs. (C2), (C4), and (16a), one finds

$$A^{11}_{qq'}(b, v_r, \Theta; \Delta) = (v_r/b)e^{-i\Delta t_c}\int_{t_c^- - t_c}^{t_c^+ - t_c} A^{11}_{qq'}(\tau, b, v_r, \Theta)e^{-i\Delta\tau}d\tau , \tag{C5}$$

where

$$A^{11}_{11}(\tau, b, v_r, \Theta) = [A^{11}_{-1-1}(\tau, b, v_r, \Theta)]^* = -3(R_x^2 - R_y^2 - 2iR_xR_y)/2R^5 , \tag{C6a}$$

$$A^{11}_{10}(\tau, b, v_r, \Theta) = A^{11}_{01}(\tau, b, v_r, \Theta) = -[A^{11}_{-10}(\tau, b, v_r, \Theta)]^*$$

$$= -[A^{11}_{0-1}(\tau, b, v_r, \Theta)] = 3R_z(R_x - iR_y)/\sqrt{2}\,R^5 , \tag{C6b}$$

$$A^{11}_{00}(\tau, b, v_r, \Theta) = (R^2 - 3R_z^2)/R^5 , \tag{C6c}$$

$$A^{11}_{1-1}(\tau, b, v_r, \Theta) = A^{11}_{-11}(\tau, b, v_r, \Theta) = \tfrac{1}{2}A^{11}_{00}(\tau, b, v_r, \Theta) . \tag{C6d}$$

The corresponding equations for the ${}^{11}A^K_Q$ defined by Eq. (14b) are

$${}^{11}A^K_Q(b, v_r, \Theta; \Delta) = (v_r/b)e^{-i\Delta t_c}\int_{t_c^- - t_c}^{t_c^+ - t_c} {}^{11}A^K_Q(\tau, b, v_r, \Theta)e^{-i\Delta\tau}d\tau , \tag{C7}$$

$${}^{11}A^0_0(\tau, b, v_r, \Theta) = 0 , \tag{C8a}$$

$${}^{11}A^1_Q(\tau, b, v_r, \Theta) = 0 \quad (Q = 1, 0, -1) , \tag{C8b}$$

$${}^{11}A^2_2(\tau, b, v_r, \Theta) = [{}^{11}A^2_{-2}(\tau, b, v_r, \Theta)]^* = -3(R_x^2 - R_y^2 - 2iR_xR_y)/2R^5 , \tag{C8c}$$

$${}^{11}A^2_1(\tau, b, v_r, \Theta) = -[{}^{11}A^2_{-1}(\tau, b, v_r, \Theta)]^* = 6R_z(R_x - iR_y)/R^5 , \tag{C8d}$$

$${}^{11}A^2_0(\tau, b, v_r, \Theta) = 3(R^2 - 3R_z^2)/6^{1/2}R^5 . \tag{C8e}$$

It should be noted that the RAIC cross sections depend only on the quantity

$${}^{pp'}_{kk'}A_{K'}(b, v_r; \Delta) = {}^{kk'}A^{K'}_{Q'}(b, v_r, \Theta; \Delta)[{}^{pp'}A^{K'}_{Q'}(b, v_r, \Theta; \Delta)]^* . \tag{C9}$$

The fact that $A_{K'}$ is independent of Θ follows directly from Eq. (15) and the orthogonality properties of the rotation matrices; from a physical viewpoint, this result is to be expected since the calculated cross sections cannot depend on the choice of the reference geometry $\Theta = 0$.

Straight-line trajectories

Under the assumption of straight-line collision trajectories, the various A's are easily calculated. Taking as a reference geometry $R_x = v\tau$, $R_y = 0$, $R_z = b$, and letting $(t_c^{\pm} - t_c) \to \pm\infty$ in Eqs. (C5) and (C7), one obtains

$$A^{11}_{11}(b, v_r, 0; \Delta) = -e^{-i\Delta t_c}\, b^{-3} \times[\alpha K_1(\alpha) - \alpha^2 K_0(\alpha)], \tag{C10a}$$

$$A^{11}_{10}(b, v_r, 0; \Delta) = -\sqrt{2}\, e^{-i\Delta t_c} b^{-3}\alpha^2 K_1(\alpha), \tag{C10b}$$

$$A_{00}^{11}(b, v_r, 0; \Delta) = -2e^{-i\Delta t_c} b^{-3} \times [\alpha^2 K_2(\alpha) - \alpha K_1(\alpha)], \quad \text{(C10c)}$$

$$^{11}A_2^2(b, v_r, 0; \Delta) = A_{11}^{11}(b, v_r, 0; \Delta), \quad \text{(C11a)}$$

$$^{11}A_1^2(b, v_r, 0; \Delta) = \sqrt{2}\, A_{10}^{11}(b, v_r, 0; \Delta), \quad \text{(C11b)}$$

$$^{11}A_0^2(b, v_r, 0; \Delta) = 3A_{10}^{11}(b, v_r, 0; \Delta)/\sqrt{6}, \quad \text{(C11c)}$$

where

$$\alpha = \Delta b / v_r \quad \text{(C12)}$$

and $K_i(\alpha)$ is a modified Bessel function. The dimensionless quantity

$$D_K(\alpha) = b^6 \sum_{\alpha} |^{11}A_Q^K(b, v_r; \Delta)|^2$$

is given by

$$D_K(\alpha) = \{2[\alpha K_1(\alpha) - \alpha^2 K_0(\alpha)]^2 + 8\alpha^4 [K_1(\alpha)]^2 + 6[\alpha^2 K_2(\alpha) - \alpha K_1(\alpha)]^2\} \delta_{K2}. \quad \text{(C13)}$$

For central tuning, $\alpha = 0$, Eq. (C13) reduces to

$$D_K(0) = 8\delta_{K2}. \quad \text{(C14)}$$

---

*Permanent address.

[1] P. R. Berman, Phys. Rev. A 22, 1838 (1980).

[2] Labels appearing on *both* sides of an equation are not to be summed over.

[3] The final-state density-matrix elements are the same whether calculated in the "normal" or the interaction representation, owing to condition (2).

[4] In RAIC I, a quantity $\Gamma_{FF_1}^{II_1}(v_r, t_c)$ was defined giving the (complex) rate at which RAIC produces a final-state density-matrix element ρ_{FF_1} from an initial one ρ_{II_1}. If Eq. (11) is multiplied by the number of collisions per unit time with the impact parameter between b and $b + db$ and relative speed v_r, and if an average over b and $\vec{R}_c$ is performed one finds

$$(\partial \rho_{FF_1}(v_r, t_c)/\partial t)_{\text{RAIC}} = \Gamma_{FF_1}^{II_1}(v_r, t_c) \rho_{II_1}(v_r, t_c),$$

where

$$\Gamma_{FF_1}^{II_1}(v_r, t_c) = \mathcal{N}_A \mathcal{N}_A v_r \int 2\pi b\, db \int d\vec{R}_c R_{FF_1}^{II_1}(b, v_r, \vec{R}_c, t_c),$$

$\mathcal{N}_\alpha$ is the α-atom density, and the $\vec{R}_c$ integral is over the atom-field interaction volume.

[5] A. R. Edmonds, *Angular Momentum Theory in Quantum Mechanics* (Princeton University Press, Princeton, N.J., 1957).

[6] In averaging over Θ, it has been assumed that all Θ are equally likely, which is equivalent to assuming a uniform distribution of relative velocities. If one or both of the atoms is velocity selected, this assumption is no longer strictly true. One can incorporate the effects of a nonuniform relative velocity distribution into the average over Θ, but the results take on a much more complicated form.

[7] The symbol $f'(f_1')$ as a superscript on $\rho_Q'^K$ is a shorthand notation for $f'J_{f'}(f'J_{f_1'})$; consequently, there is no summation on $J_{f'}$ or $J_{f_1'}$ in Eqs. (23).

[8] M. G. Payne, V. E. Anderson, and J. E. Turner, Phys. Rev. A 20, 1032 (1979); E. J. Robinson, J. Phys. B 13, 2359 (1980).

[9] S. Haroche, in *High Resolution Laser Spectroscopy*, edited by K. Shimoda (Springer, Berlin, 1976), pp. 275–279.

[10] S. E. Harris, J. F. Young, W. R. Green, R. W. Falcone, J. Lukasik, J. C. White, J. R. Willison, M. D. Wright, and G. A. Zdasiuk, in *Laser Spectroscopy IV*, edited by H. Walther and K. W. Rothe (Springer, Berlin, 1979), p. 349 and references therein; C. Bréchignac, Ph. Cahuzac, and P. E. Toschek, Phys. Rev. A 21, 1969 (1980).